Article

Current Biology

Compound starch granule formation in grass seeds is associated with distinct temporal patterns of gene expression

Graphical abstract

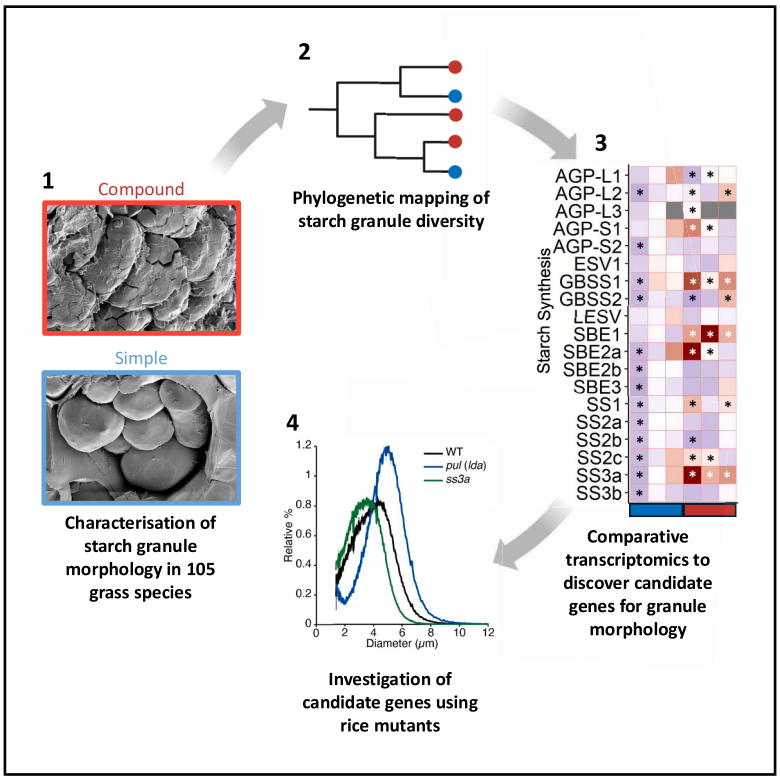

Highlights

- Survey of 105 Pooideae species for variation in seed starch granule morphology
- There were multiple evolutionary transitions between simple and compound granules
- Starch content and polymer structure cannot distinguish simple and compound granules
- Comparative transcriptomics reveals candidate genes for compound-granule formation

Authors

Alexander Watson-Lazowski, Doreen Feike, Qi Yang Ngai, ..., Ryo Matsushima, Alison M. Smith, David Seung

Correspondence

awatsonlazowski@harper-adams.ac.uk (A.W.-L.), david.seung@jic.ac.uk (D.S.)

In brief

Watson-Lazowski et al. survey seed starch granule morphology in 105 Pooideae grasses, showing the phylogenetic distribution of simple and compound starch granules, the two major morphological classes. Transcriptomics analysis associates compound-granule formation with distinct gene expression patterns during seed development, revealing several candidate genes involved in the process.

Watson-Lazowski et al., 2026, Current Biology *36*, 1142–1155
March 9, 2026
https://doi.org/10.1016/j.cub.2026.01.038

CellPress

CellPress
OPEN ACCESS

Current Biology

Article

Compound starch granule formation in grass seeds is associated with distinct temporal patterns of gene expression

Alexander Watson-Lazowski,[1,2,*] Doreen Feike,[1] Qi Yang Ngai,[1] Lara Esch,[1,5] Naoko Fujita,[3] Ryo Matsushima,[4] Alison M. Smith,[1] and David Seung[1,6,*]

[1]John Innes Centre, Norwich Research Park, Norwich NR4 7UK, UK
[2]Harper Adams University, Newport TF10 8NB, UK
[3]Department of Biological Production, Akita Prefectural University, 241-438 Kaidobata-nishi, Shimoshinjo-nakano, Akita, Akita 010-0195, Japan
[4]Institute of Plant Science and Resources, Okayama University, 2-20-1 Chuo, Kurashiki, Okayama 710-0046, Japan
[5]Present address: Institute of Plant Science, The University of Edinburgh, The Kings Buildings, EH9 3BF Edinburgh, UK
[6]Lead contact
*Correspondence: awatsonlazowski@harper-adams.ac.uk (A.W.-L.), david.seung@jic.ac.uk (D.S.)
https://doi.org/10.1016/j.cub.2026.01.038

SUMMARY

There is extensive interspecies variation in starch granule morphology in the endosperm of grass species, but the factors underpinning this variation are poorly understood. The two major granule morphology types among species are simple and compound granules, where simple granules arise from a single initiation per amyloplast, and compound granules form from multiple granule initiations. Here, we carried out an extensive survey of seed starch morphology, examining specimens from 105 species within the Pooideae using electron microscopy. This not only expanded our current knowledge of the diversity of starch granule types but also confirmed the homoplasy of simple and compound starch granules. We then selected species representing independent origins of simple (*Brachyelytrum japonicum*, *Phaenosperma globosa*, and *Brachypodium distachyon*) and compound granules (*Nardus stricta*, *Melica altissima*, and *Calamagrostis brachytricha*) for analysis of starch structure and gene expression. There were no clear patterns in starch content, amylopectin structure, or amylose content that could distinguish the two granule types. However, comparative transcriptomics over seed development revealed gene expression patterns associated with granule type, most notably increasing expression of *STARCH SYNTHASE 3a* (SS3a), *STARCH BRANCHING ENZYME 1* (SBE1), and limit dextrinases (LDAs) between 3 and 9 days post anthesis in species with compound granules. Mutation of these genes in rice, which natively produces compound granules, resulted in altered granule shape and/or size. Our work highlights differences in gene expression that could contribute to natural variation in granule morphology within the Pooideae while providing important new starch phenotype and gene expression datasets that can be widely used to study endosperm development.

INTRODUCTION

Starch plays an integral role in plant physiology and is also vital for human nutrition.[1] It consists of two glucose polymers: amylopectin is highly branched, consisting of α-1,4-linked linear chains with α-1,6-linked branches, whereas amylose is primarily α-1,4-linked linear chains. The two polymers together form semi-crystalline starch granules, and the morphology of these granules is among the major factors influencing starch functionality and digestibility.[2–4]

There is vast diversity in the morphology of starch granules across species, the origin of which is poorly understood.[5–7] For example, grass species (Poaceae) can be categorized according to granule morphology in the endosperm, which is linked to the spatiotemporal pattern by which the granules are initiated during grain development.[7,8] The categories include (1) "simple," where each granule arises from a single initiation within each amyloplast (e.g., maize)[9,10]; (2) "compound," where multiple granules initiate within each amyloplast and grow into a tessellated structure, creating polygonal granules (e.g., rice); and (3) "bimodal," where a large A-type granule with flattened morphology initiates in each amyloplast early in seed development, and small, spherical B-type granules initiate later in amyloplast stromules (e.g., wheat and barley).[8,11,12] In addition, some species (e.g., oat) produce both simple and compound granules,[13,14] and others have a liquid, soft, or semi-soft endosperm at maturity for which there is no information on granule morphology.[15,16] Whereas the presence of bimodal granules appears to be restricted to the Triticeae, there are no obvious phylogenetic trends on the occurrence of the other granule morphology types. This suggests that simple and compound granules have numerous independent evolutionary origins or transitions.[3,8]

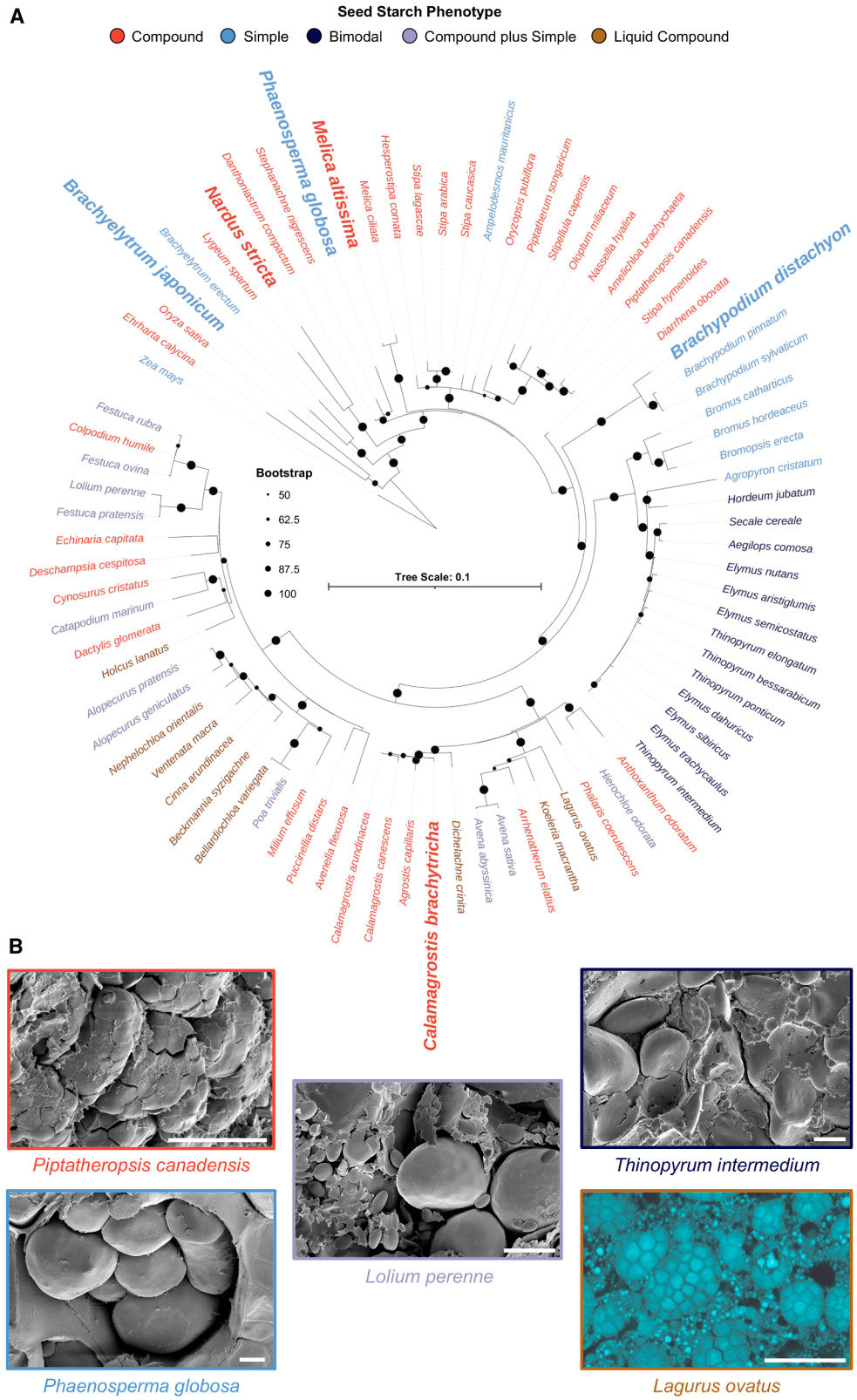

Figure 1. Starch granule diversity across the Pooideae subfamily

(A) Maximum likelihood phylogenetic tree of species across the Pooideae subfamily, color coded based on their seed starch granule phenotype. The tree was built using partial sequences of *matk* and *ndhF*, and *Zea mays* is used as the root of the tree. *Zea mays*, *Ehrharta calycina*, and *Oryza sativa* were used to root the

(legend continued on next page)

Several mutations are known to affect endosperm starch granule morphology, including those in proteins involved in granule initiation—the process that determines the number of granules per amyloplast. STARCH SYNTHASE 4 (SS4) and its interaction partner PROTEIN TARGETING TO STARCH 2 (PTST2) are key components involved in starch initiation.[17] Loss of PTST2 (also known as B-GRANULE CONTENT 1 [BGC1] in wheat and FLOURY ENDOSPERM 6 in barley and rice) induces supernumerary granule initiations per amyloplast and the subsequent formation of compound-like granules in the endosperm of *Brachypodium*, barley, and wheat—species that normally make simple or bimodal granules.[18–21] Similar compound granules have been observed in wheat mutants defective in SS4.[19] Additionally, some mutations in genes typically associated with amylopectin biosynthesis can also influence granule morphology. Linear amylopectin chains are extended by STARCH SYNTHASE isoforms (SS1–3), while BRANCHING ENZYME (BE) isoforms introduce the branches. Rice mutants deficient in *STARCH SYNTHASE 3a* (SS3a) accumulate granules that appear rounded, resembling simple granules.[22] This effect is enhanced by the additional elimination of SS4b.[23] In addition to SS and BE isoforms, debranching enzymes are required for proper amylopectin synthesis—primarily isoamylases (ISAs) and, to some extent, limit dextrinases (LDAs). Barley mutants deficient in isoamylase 1 (ISA1) also form compound-like granules.[24]

These mutant phenotypes raise the possibility that variation between species in the relative amounts and expression patterns of amylopectin-synthesizing enzymes and/or initiation proteins might be responsible for the wide interspecific differences in granule morphology. However, variation in these proteins alone cannot fully account for natural variation in granule morphology. For example, even though loss of PTST2 and ISA1 can induce compound-granule formation in barley,[20,24] rice produces compound granules despite having functional PTST2 and ISA1, and rice mutants in either gene have other defects in starch synthesis.[25,26]

Here, we aimed to characterize granule morphology in a diverse seed collection of 105 grass species and elucidate the differences in gene expression during seed development that could underpin different granule morphology. We reveal common gene expression patterns and multiple candidate genes associated with simple vs. compound granules, suggesting that variation between species in granule initiation and morphology is likely to have complex origins.

RESULTS

Diversity of starch granule morphology across the Pooideae subfamily

To study starch granule morphology in wild grass species, we obtained mature seeds of 105 diverse species within the Pooideae and completed a detailed survey of granule morphology using scanning electron microscopy. Capturing the diversity within a single study using the same imaging approach greatly extends the existing information on the diversity of starch morphology in grass species collated by Matsushima et al.,[8] which was based on information collected across multiple individual studies. Representative images for all species are provided in Data S1, while the classifications made were recorded in Table S1. Further, for 78 species where data were available, we extracted *matk* and *ndhF* genomic sequences to build a phylogenetic tree, and we visualized the distribution of the different granule morphologies on the tree (Figure 1A). Most species had granules that were simple, compound, or bimodal. The distribution of simple and compound granules within the Pooideae showed multiple independent origins of the two morphological types. Species with bimodal granule morphology (defined as A- and B-type granules) were confined to the Triticeae, suggesting a single origin of bimodal granules within this tribe. One exception was *Agropyron cristatum*, which is in the Triticeae but did not contain B-type granules.

We identified 13 species that had both compound and simple granules (classed as "compound plus simple"), from which all but one (*Ptilagrostis mongholica*) belonged to the two major clades of the Poeae tribe (chloroplast groups 1 and 2) (Table S1). Additionally, nine species had a liquid endosperm that was not firm at maturity. These species were exclusively found in the chloroplast groups 1 and 2 clades of the Poeae. As liquid samples cannot be viewed with electron microscopy, we used light microscopy to visualize granules in four species representing independent occurrences of the liquid endosperm trait. In all four cases, we observed compound granules within the liquid endosperms, so we classified these as "liquid compound" (Figure S1). Notably, all of the 43 species analyzed within the Poeae had at least some compound-granule formation (Table S1). However, the presence of compound-plus-simple and liquid-compound morphologies suggests that variations on compound-granule morphology arose multiple times independently, primarily within the Poeae.

Given that simple and compound granules were the most prevalent granule morphology types with multiple independent origins, we selected for further characterization three species that produce simple granules (*Brachyelytrum japonicum*, *Phaenosperma globosa*, and *Brachypodium distachyon*) and three that produce compound granules (*Nardus stricta*, *Melica altissima*, and *Calamagrostis brachytricha*). These were selected because they are phylogenetically distinct from each other (Figure 1A), representing independent evolutionary transitions between simple and compound granules. The plants also grew well under our growth conditions and reliably produced seeds.

Seed development, morphology, starch content, and polymer structure

We examined developing seeds of the six selected species, collected at 3, 6, 9, and 14 days post anthesis (DPA)

phylogenetic tree but are not part of the Pooideae subfamily. Colors represent endosperm starch granule phenotype. Where no dot is present on a branch, the bootstrap support for the branch is below 50. Species in large bold font are those selected for further investigation.
(B) Examples of scanning electron micrographs (or confocal images post staining with safranin O in the case of liquid compounds) showing each type of granule morphology. Scale bars, 10 μm.
See also Figure S1, Data S1, and Table S1.

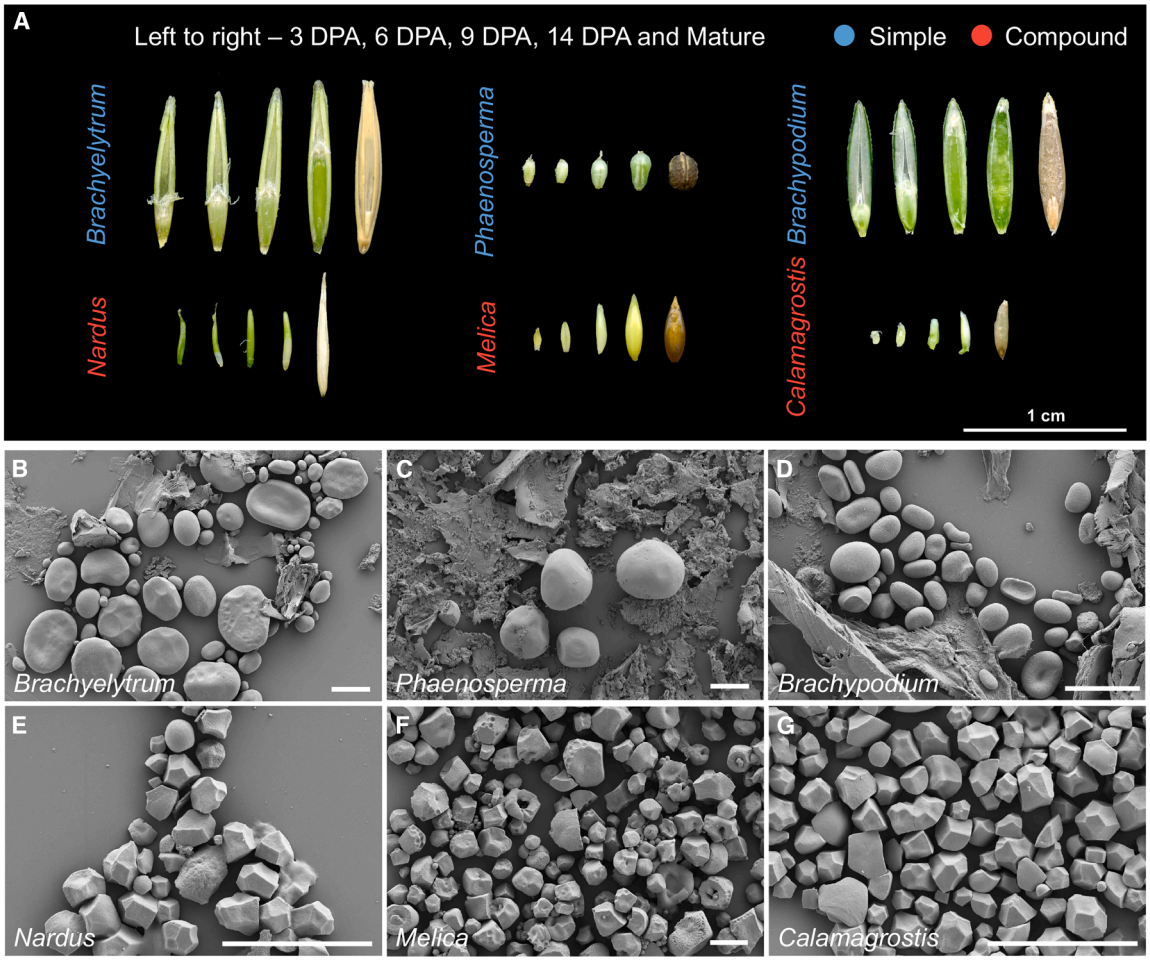

Figure 2. Seed development and starch granule morphologies for simple and compound species

(A) Images of seeds through development (3, 6, 9, and 14 days post anthesis [DPA]) for each species. Scale bar, 1 cm.

(B–G) Examples of scanning electron micrographs of purified starch from mature seeds of (B) *Brachyelytrum japonicum*, (C) *Phaenosperma globosa*, (D) *Brachypodium distachyon*, (E) *Nardus stricta*, (F) *Melica altissima*, and (G) *Calamagrostis brachytricha*. Scale bars, 10 μm.

See also Figure S2.

(Figure 2A). Microscopy of cross-sectioned seeds confirmed that these time points effectively captured endosperm development, granule initiation, and starch accumulation in all species (Figure S2). Scanning electron microscopy on starch purified from mature seeds showed rounded granules in all simple species and polygonal granules in all compound species, confirming starch morphology type for each species (Figures 2B–2G).

We investigated whether starch content and polymer structure in mature seeds differed between species with simple and compound granules. Overall, we observed no correlation between the occurrence of simple or compound granules and total starch content, amylose content, and amylopectin chain length distribution, although there were differences in these factors between species (Figure 3). *Brachypodium* had the lowest seed starch content, consistent with the low starch contents previously reported for the species,[18,27] while *Melica* had the highest (Figure 3A). *Phaenosperma* had the highest amylose content at ~50%, while the other species had amylose contents within the range reported for most cereals (~20%–35%) (Figure 3B). Amylopectin chain length distributions were similar for all species except that peak chain length was at degree of polymerization (dp) 16–20 in *Melica* and *Phaenosperma*, while it was at dp 10–12 in the other species (Figure 3C).

Granule-specific transcript expression patterns over seed development

To investigate whether simple- and compound-granule species differed from each other with respect to transcriptional changes during endosperm development, RNA sequencing (RNA-seq) was carried out at time points 3, 6, 9, and 14 DPA for each species except *Nardus*, where only time points 3 and 9 DPA were used due to limited material. A clustering approach was used to define conserved trends of transcript expression over seed development and to identify any trends specific to compound-granule or simple-granule species (Figure 4). Clustering was carried out on transcripts from all species (Figure 4A), simple-granule species only (Figure 4B), and compound-granule species only (Figure 4C). Clusters for all species and simple-granule

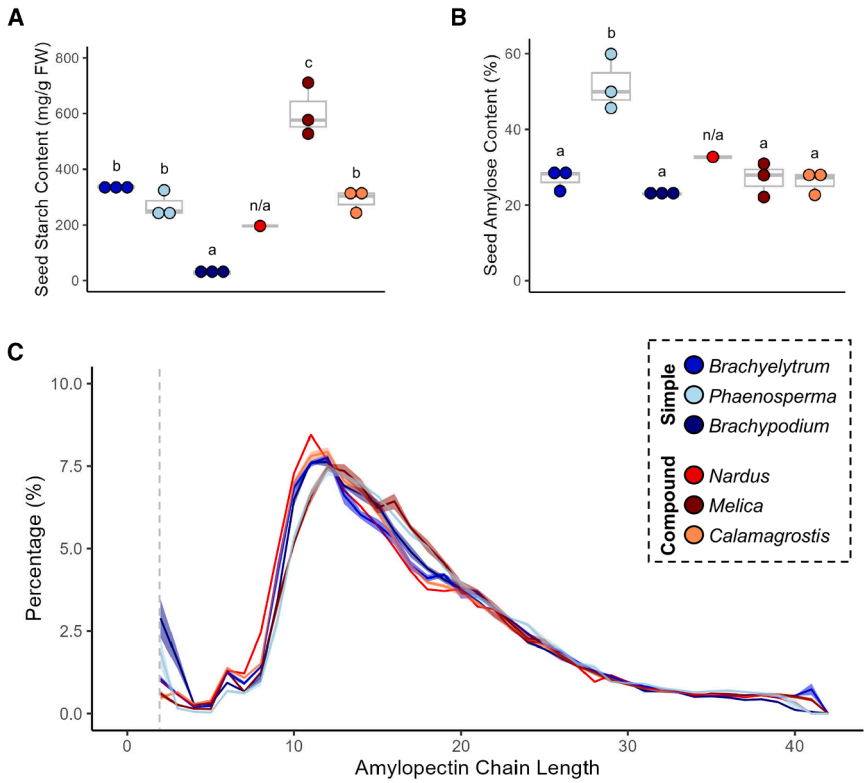

Figure 3. Characteristics of simple and compound starches

(A) Starch content, (B) amylose content, and (C) amylopectin branch length distribution were determined in mature seeds. Each measurement used three biological replicates ($n = 3$), each representing a measurement made on separate plants. An exception is *Nardus stricta*, for which the three biological replicates were pooled for each measurement due to limited material. Thus, *Nardus* was omitted from the statistical analyses (labeled n/a). Significance is indicated where two letters differ ($p \leq 0.05$), calculated using a one-way ANOVA and a Tukey's post hoc test.

species represented general upward (all species C3 and simple C2) or downward (all species C1, C2, and simple C1) trends over seed development. Clusters for compound-granule species also showed general upward trends (compound C2 and C3) and downward (compound C4 and C5) trends but had an additional cluster with a distinct zig-zag pattern across development (compound C1). Compound C1 was unique because the expression levels at the three later time points first rise above and then fall below the level observed at 3 DPA, whereas expression levels in the other clusters stay consistently above or below the 3 DPA level. The presence of two clusters with generally upward trends for compound-granule species (compound 2 and 3) but only one upward-trending cluster for all species and simple-granule species (all species C3 and simple C2) prompted us to examine transcripts underlying these clusters. The overlap of the clusters was used to identify transcripts unique to each cluster (Figure 4D). Gene Ontology (GO) enrichment of the 814, 933, and 581 transcripts unique to simple C2, compound C2, and compound C3, respectively, revealed a significant overrepresentation (adj. $p \leq 0.05$) of two carbohydrate-related transcript categories in compound C3, "carbohydrate metabolic process" and "glycogen debranching enzyme activity," which include enzymes involved in starch metabolism (Figure 4E).

A statistical approach was used to further investigate differences in transcript levels over seed development. Species differed greatly in the numbers of transcripts that were significantly differentially expressed (DE) (false discovery rate [FDR] ≤ 0.05) between developmental stages (Table 1). In three species, the sum of the transcripts that were DE when comparing all developmental stages was large (*Brachypodium*, *Melica*, and *Calamagrostis*: 14,649, 10,981, and 6,827 unique transcripts, respectively), while far fewer transcripts were DE between developmental stages in *Phaenosperma*, *Nardus*, and *Brachyelytrum* (1,386, 469, and 56 unique transcripts, respectively; note: only one pair of time points could be compared for *Nardus*). These patterns were not specifically associated with either simple or compound-granule formation and may be linked to other features of seed development, such as seed size, number, and maturation rate. Heterogeneity of biological replicates may also account for some of the general transcriptomic variability seen between species (Figure S3).

Despite limitations on analysis imposed by the large transcriptomic variability between species (based on numbers of DE transcripts identified), DE transcripts were identified that exhibited a conserved expression pattern (DE in the same direction) between periods of seed development in compound-granule species only (compound-granule specific; Table 1). GO enrichment analysis revealed that GO categories related to starch metabolism were significantly overrepresented (adj. $p \leq 0.05$) among the upregulated compound-granule-specific DE transcripts (Data S2). GO categories related to starch were significantly overrepresented within two comparisons over seed development but were particularly apparent (and accounted for almost all the GO categories identified) within the compound-granule-specific upregulated DE transcripts when comparing 3 to 9 DPA. Among downregulated compound-granule-specific DE transcripts, fewer GO categories were identified, and these were not directly related to starch metabolism.

Distinct patterns of transcript abundance for starch-related genes in compound-granule species

For all six species, we examined changes in abundance over development of DE transcripts related to starch and sugar metabolism (Figures 5 and S4). We made this analysis over the 3- to 9-DPA interval because data were available for all six species, and there were DE transcripts relating to several starch-related GO categories (Data S2). Among the 19 genes related to starch synthesis, none showed significant differences in two or more

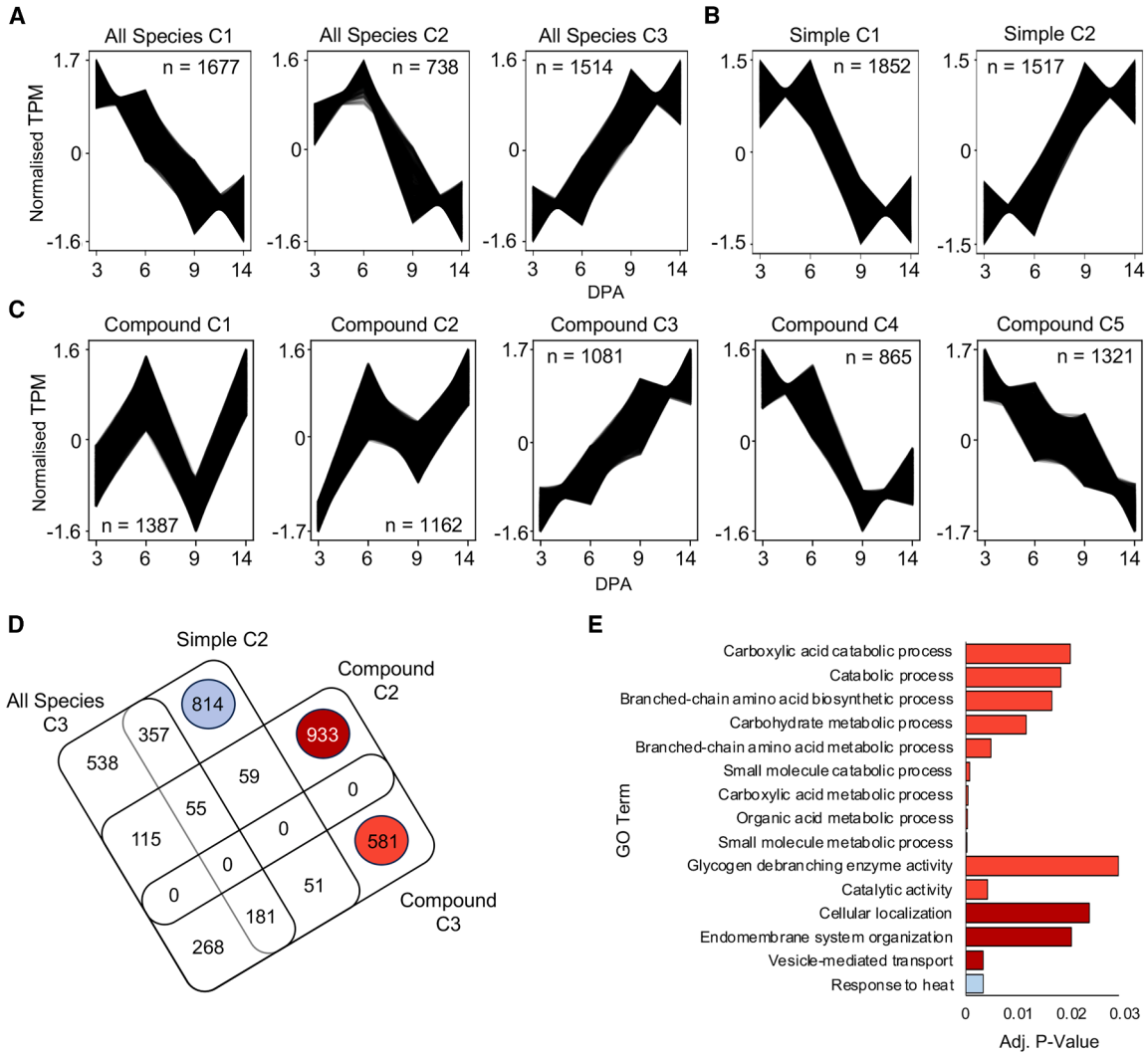

Figure 4. Clustering analysis of transcript data over seed development

(A–C) Clustering analysis of transcripts (post-filtering) over seed development from 3 to 14 days post anthesis (DPA) using *Clust*. (A) All species (*Brachyelytrum japonicum*, *Phaenosperma globosa*, *Brachypodium distachyon*, *Nardus stricta*, *Melica altissima*, and *Calamagrostis brachytricha*), (B) simple-granule species only (*Brachyelytrum*, *Phaenosperma*, and *Brachypodium*), and (C) compound-granule species only (*Nardus*, *Melica*, and *Calamagrostis*). Transcript abundance was normalized as normalized transcripts per million (TPM) prior to clustering using in-built normalization protocols.

(D) The overlap of all clusters with upward trends over development. Values are numbers of transcripts in each category.

(E) Significantly overrepresented (adj. $p \leq 0.05$) molecular function and biological process GO categories that are specific to each upregulated cluster (as identified in D). The colors of the bars correspond to the cluster to which they are specific (blue, simple C2; dark red, compound C2; and light red, compound C3). A list of the corresponding *Brachypodium* accession numbers contained in each cluster, and the full list of significantly overrepresented GO categories, can be found in Data S2.

See also Figures S3 and S4.

species in the simple-granule type, whereas as many as 10 did in the compound-granule types.

The major finding from this analysis was that the abundance of several transcripts associated with starch synthesis and degradation significantly rose between 3 and 9 DPA (FDR $\leq$ 0.05) in all compound-granule species but did not rise in simple-granule species (Figures 5B and 5C). This makes them candidates for involvement in compound-granule formation. These genes were SS3a, *STARCH BRANCHING ENZYME 1* (SBE1), and LDA. Transcripts for the gene encoding the amylose-synthesizing enzyme GRANULE BOUND STARCH SYNTHASE 1 (GBSS1) were also upregulated between 3 and 9 DPA in all compound-granule species. However, given that the amylose content of starch did not differ between simple- and compound-granule species (Figure 3), the *GBSS1* gene was deprioritized for further characterization.

Transcripts related to granule initiation (Figure 5A) and starch degradation showed no patterns of change specific to compound or simple granules, although there were some striking differences between species: for example, a strong upregulation

Table 1. Significantly DE transcripts over seed development

	3 vs. 6 DPA		3 vs. 9 DPA		3 vs. 14 DPA		6 vs. 9 DPA		6 vs. 14 DPA		9 vs. 14 DPA	
	Up	Down	Up	Down	Up	Down	Up	Down	Up	Down	Up	Down
Brachypodium	1,969	1,961	5,015	5,206	5,106	5,175	5,032	4,557	5,331	4,717	196	15
Phaenosperma	2	0	9	1	725	625	0	0	163	319	127	166
Brachyelytrum	0	1	27	28	0	0	0	0	0	0	0	0
Melica	619	367	3,501	3,304	4,431	4,111	2,324	1,530	3,946	2,758	1,066	749
Calamagrostis	654	71	3,644	2,197	2,390	2,154	70	107	18	174	2	2
Nardus	N/A	N/A	172	297	N/A	N/A	N/A	N/A	N/A	N/A	N/A	N/A
Simple species only	0	0	0	0	0	0	0	0	0	0	0	0
Compound species only	84	3	12	2	396	277	1	9	0	21	0	0
All species	0	0	0	0	0	0	0	0	0	0	0	0

Values represent the numbers of annotated significantly DE transcripts (FDR $\leq$ 0.05; fold change $\geq$ 1.5) for each time interval over seed development. In the upper part of the table, numbers are shown for each species. The lower part of the table shows numbers of DE genes that were common among all simple species, all compound species, or all species. Comparisons that could not be made due to the relevant time points not being sampled are marked with N/A. See also Data S2.

(FDR $\leq$ 0.05) of *MYOSIN-RESEMBLING CHLOROPLAST PROTEIN* (MRC) in *Calamagrostis*. Our analysis did not include STARCH SYNTHASE 5 (SS5), a protein that influences granule size and number in Arabidopsis leaves, because it is absent from *Brachypodium*.[28] However, examination of our *de novo* transcript assemblies revealed that only *Brachyelytrum* and *Nardus* had detectable SS5 orthologs, so presence/absence of SS5 cannot differentiate the two granule types. There were also no differences in patterns of transcripts related to sugar metabolism that could differentiate the granule types (Figure S4).

Mutant lines of rice lacking expression of SS3a, SBE1, or LDA have altered granule morphology

Validating the role of our candidate genes *SS3a*, *SBE1*, or *LDA* in compound-granule formation in our selected species is challenging, as none of our compound-granule-producing species are amenable to genetic transformation. However, rice (*Oryza sativa*) has compound granules that are similar to those in the Pooideae, and mutants are available in all three candidate genes. We first observed sections of mature grains from the rice mutants using light microscopy (Figure 6A). All three mutants had compound granules as the major granule type, suggesting that loss of any one of the three candidate genes does not cause a full transition to simple granules. However, as previously reported,[23] the *ss3a* mutant showed defective compound-granule organization. The *ss3a* compound granules were smaller than those of the wild type, with many containing only a few granules, and there were some small granules that were not obviously associated with a compound granule. There were no obvious defects in compound-granule formation in mutants defective in SBE1 or PULLULANASE (PUL; the ortholog of LDA in rice). We also analyzed the morphology of purified granules using scanning electron microscopy. All three mutant lines primarily produced polygonal granules, although some rounded simple granules were observed for *ss3a* (Figure S5).

Since granule size is a major parameter of granule morphology that can be accurately quantified, we analyzed granule size distributions using a Coulter counter. Given that none of the three mutants have significant changes in starch content,[22,29,30] we reasoned that changes in granule size could reflect changes in granule number per plastid. We observed strong alterations in granule size distributions in both *ss3a* and *pul* (*lda*) mutants, where the *ss3a* had decreased granule size relative to the wild type, and *pul* (*lda*) had increased granule size (Figure 6B). A more subtle change in the granule size was observed in the *sbe1* mutant (Figure 6C). To analyze statistical significance, we calculated the relative number of granules falling within three size bins. The proportion of small granules (<3 μm) significantly decreased in the *pul* (*lda*) and *sbe1* mutant relative to their wild-type controls, and the proportion of medium-sized granules (3–6 μm) significantly increased (Figure 6D). The relative number of large granules (>6 μm) significantly increased in the *pul* (*lda*) mutant relative to the wild type but not in the *sbe1* mutant. Overall, this suggests that there was a significant shift toward larger granule sizes in both *pul* (*lda*) and *sbe1* mutants, where the *pul* (*lda*) has a stronger increase than *sbe1*. By contrast, there was a strong shift toward smaller granules in the *ss3a* mutant, with the mutant having significantly more small granules and fewer medium and large granules than the wild type. Thus, all three genes influence granule morphology in rice, with SS3a and PUL (LDA) having the strongest influence on compound-granule formation.

DISCUSSION

Understanding diversity in starch granule formation within the Pooideae

Our study provides new insights into the morphological diversity of starch granules within the Pooideae and reveals the gene expression signatures that distinguish the two major morphological classes (simple vs. compound granules). Our phenotypic and transcriptomics datasets provide an important resource for studying starch and endosperm development in wild grass species.

Our survey of granule morphology builds upon the previous survey of granule morphology curated by Matsushima et al.[8] by using electron microscopy to examine starch granules at high resolution for all species within a single study, distinguishing

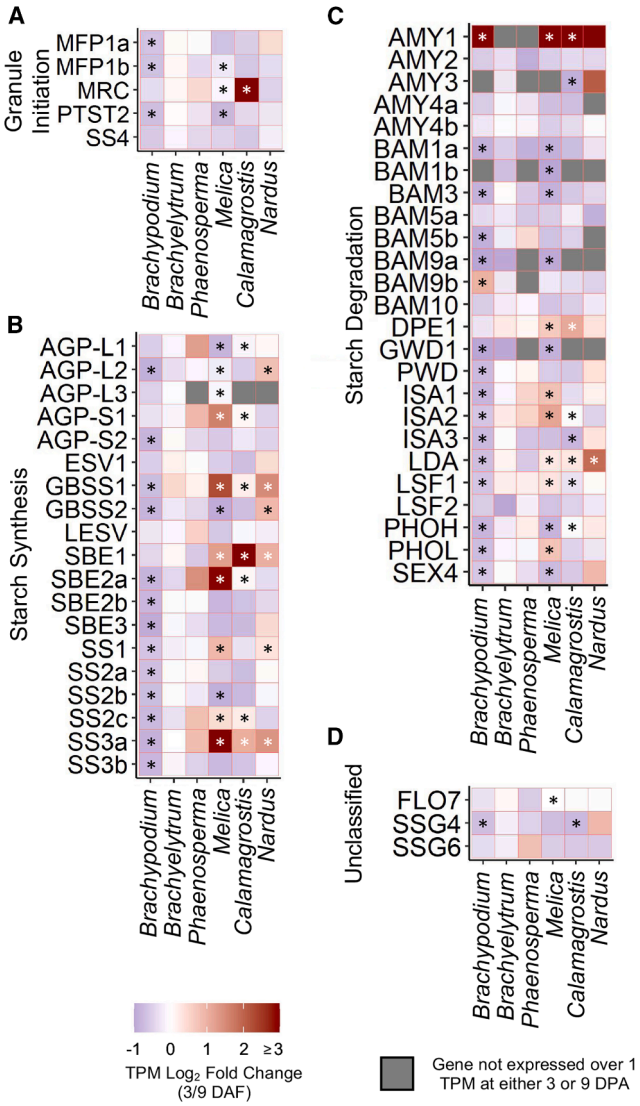

Figure 5. Changes in transcript abundance for genes encoding proteins of starch metabolism during seed development

Transcript per million (TPM) $\log_2$ fold change (between 3 and 9 DPA) for (A) starch granule initiation, (B) starch synthesis, (C) starch degradation, and (D) unclassified starch-related genes. White or black asterisks highlight where a transcript was significantly DE (FDR $\leq$ 0.05) across the two time points. A list of the corresponding *Brachypodium distachyon* accession numbers for each gene can be found in Table S2.

more granule morphology types, and exploring tribes where information on starch was not available. Our findings are largely consistent with the previous study regarding the homoplastic distribution of simple and compound granules. However, there were also new insights into the morphological diversity.

Firstly, we observed a more widespread occurrence of species with both simple and compound granules within the same endosperm. This mixed granule type was previously reported for oat (*Avena sativa*) and for several non-Pooideae species in the PACMAD clade,[8,14] but we identified 13 Pooideae species with this configuration (Table S1). *Alopecurus* and *Poa* genera were previously classified as having compound granules, but the species examined here (*Alopecurus geniculatus*, *Alopecurus pratensis*, and *Poa trivialis*) had mixed simple and compound granules. Interestingly, almost all species with this mixed granule type fell into both clades of the Poeae (chloroplast groups 1 and 2), suggesting that the trait was more common in this tribe. The exception was *Ptilagrostis mongholica* in the Stipeae tribe—for which all other species examined had exclusively compound granules (Table S1). It is possible that our high-resolution imaging allowed us to more accurately detect the co-occurrence of simple granules within these species, or that there are differences between the species/accessions that we examined compared with previous works.

Secondly, our classification defined bimodal strictly as the presence of flattened A-type and round B-type granules, which was found only in the Triticeae. Our justification for this definition is that many species outside the grasses contain sub-populations of large and small granules, which are clearly different from the morphologically distinct A- and B-type granules that accumulate in the Triticeae endosperm. A notable exception in our dataset was *Agropyron cristatum* (Triticeae), which did not contain B-type granules. It is known that some members of the *Aegilops* genus (Triticeae) have also lost B-type granules.[31,32] Therefore, combined with *Aegilops*, our data on *Agropyron* suggest at least two independent losses of B-type granules within Triticeae evolution.

Finally, our seed collection contained nine species that had a liquid/gel-like endosperm. Liquid endosperms have previously been noted within the Pooideae,[15,33] but the starch phenotype within such endosperms was unknown. We discovered that four diverse representatives of these species contained compound granules (Figure S1; Table S1). The liquid endosperms were only found in the Poeae, suggesting the evolution of novel endosperm traits within this tribe.

Such remarkable diversity naturally raises questions about the adaptive significance of different starch morphology types. It is not known whether simple or compound granules confer a competitive advantage under various biotic or abiotic conditions. However, it is tempting to speculate that distinct granule shapes and sizes could optimize seed packing or starch digestion rates during germination. Alternatively, the variation may persist within grass endosperms because no single morphology type offers a clear advantage over the others. Our study provides a foundation for further physiological and ecological research to test these hypotheses.

Diverse species with the same starch granule phenotype have similar temporal expression patterns

The influence of granule morphology (particularly granule size) on nutritional and functional properties of starch provides strong rationale to study mechanisms influencing granule morphology.[2,4] Although granule morphology has been well characterized in major crop cereals such as maize (simple), rice (compound), wheat (bimodal), and oat (compound plus simple),[6] these provide only a single representative species for each class, making it difficult to study general commonalities and differences between the morphology classes. The advantage of using wild grass species in our study is that multiple examples of simple- or compound-granule-producing species from

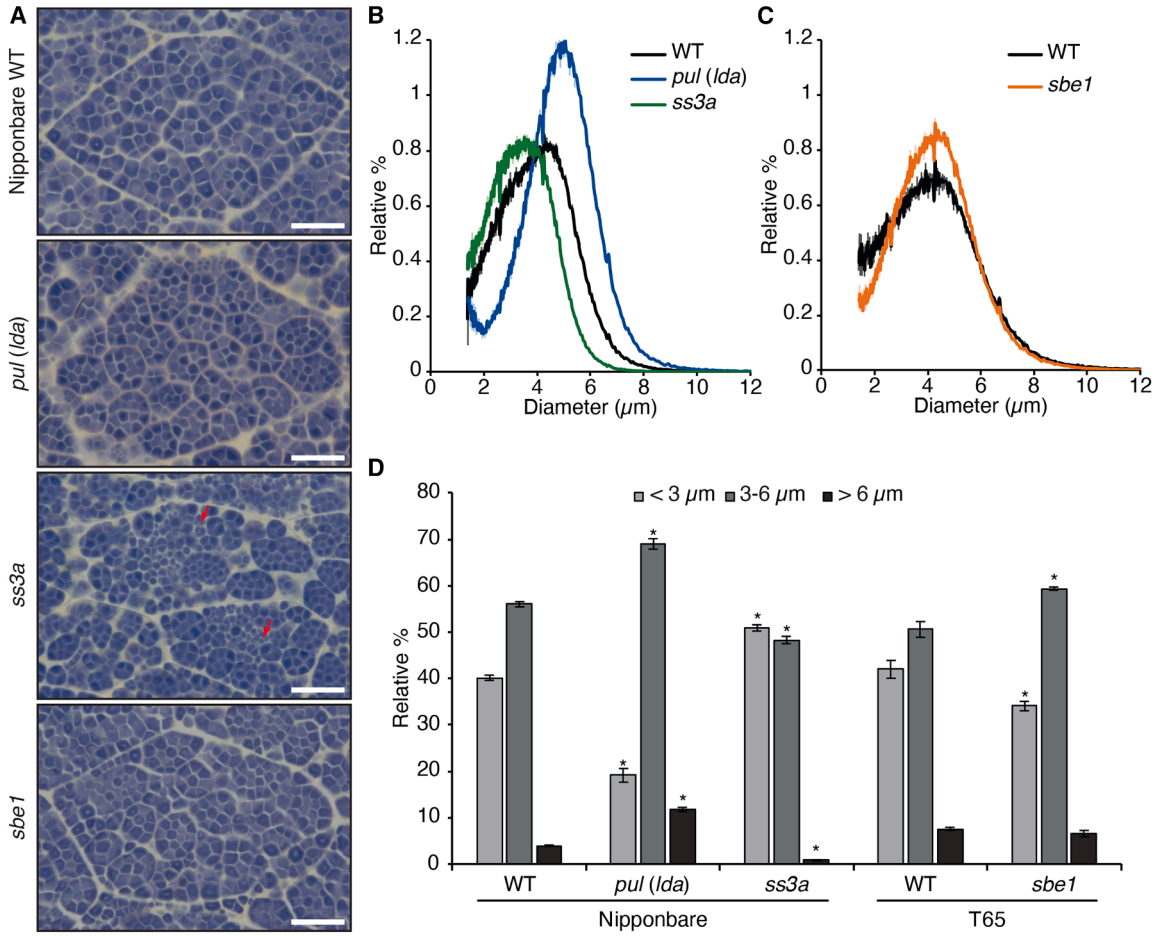

Figure 6. Rice mutants defective in candidate genes have altered starch granule morphology

(A) Light micrographs of thin sections prepared from mature grains of rice *sbe1*, *ss3a*, and *pul* (*lda*) mutants. Examples of small compound granules in the *ss3a* mutant are marked with arrows.

(B and C) Granule size distributions measured on the Coulter counter. (B) Size distributions for *pul* (*lda*) and *ss3a* mutant and wild-type (WT, Nipponbare) granules. (C) Granule size distribution for *sbe1* and WT (T65) granules. For both panels, the solid line represents the mean from $n = 3$ replicate measurements on the same starch preparation, which was extracted from a pool of 200 grains, and the shading indicates the SEM.

(D) Mean starch granule size, calculated as the average particle size from the distributions shown in (B) and (C). Values are the mean ± SEM of the $n = 3$ replicate measurements. An asterisk indicates a significant difference ($p \leq 0.05$) between the mutant and the relevant WT for that starch granule size bin, using a one-way ANOVA and Tukey's post hoc test for Nipponbare genotypes and a pairwise *t* test for T65 genotypes.

See also Figure S5.

independent lineages could be examined. Analysis of seed size, starch content, amylose content, and amylopectin structure showed no consistent differences between simple and compound granules in the species examined (Figure 2). The lack of general differences in these other starch/seed properties suggests that granule morphology is the main distinguishing factor between the simple- and compound-granule-producing species, allowing the observed patterns in gene expression to be linked to granule morphology rather than other properties.

Due to the phylogenetic distance of the species used, there were large differences in the gene expression patterns between species. However, there were distinct expression profiles that were specific to compound-granule-forming species. Many genes exhibited compound-specific expression patterns across development. The most interesting subset was apparent within genes that were upregulated between 3 and 9 DPA time points, where there was overrepresentation of several carbohydrate and starch-related GO categories in compound-granule-forming species. These expression differences during these early developmental time points coincided with when the initiation of granules took place in the endosperm (Figure S2). As simple vs. compound granules result from differences in the number of initiations in the amyloplast,[34] we would expect the most relevant differences in gene expression that differentiate the two granule morphology types to happen within this early developmental time frame. In addition, expression pattern clusters over development were more dynamic in compound-granule species compared with simple-granule species (Figure 4), suggesting that the formation of compound granules may require a more complex regulation of genes over seed development.

Within the compound-specific clusters showing increased expression over seed development, the cluster (compound C3) with a large increase in expression between 3 and 9 DPA was noted as containing carbohydrate-related genes, which is consistent with the findings from the individual comparisons mentioned above.

Compound-granule formation is associated with distinct expression patterns of known starch genes

Due to the prevalence of carbohydrate-related genes in the 3 vs. 9 DPA comparison (Data S2), known carbohydrate metabolism genes were investigated within this comparison to identify which genes were driving the above responses (Figure 5). Surprisingly, none of the known granule initiation genes exhibited simple or compound-specific expression patterns. Loss-of-function mutations in PTST2, SS4, or ISA1 can induce the formation of compound granules in the endosperm of species that normally make simple (e.g., *Brachypodium*[18]) or bimodal granule types (e.g., barley[20,24] and wheat[19,21]). However, PTST2 and SS4 had similar expression patterns in all species analyzed, and while ISA1 showed some species-specific differences, these were not consistent within either granule type.

Rather, SS3a, SBE1, and LDA were identified as candidate genes involved in compound-granule formation. These genes significantly increased in expression in all three compound-granule-producing species across 3–9 DPA, while simple-granule-producing species either had significantly downregulated expression or exhibited no significant change over the same time points. Although all three genes are not categorized as "granule initiation" genes, it is plausible that all three are involved in the compound-granule formation process.

SS3a is a particularly strong candidate gene for compound-granule formation. Grasses have two paralogs of SS3 (SS3a and SS3b), and SS3a is predominantly expressed in the endosperm of rice.[35] Rice mutants deficient in the enzyme accumulate small granules without major changes in total starch content, some of which have rounded, simple-granule morphology[22] (Figure 6). The formation of simple granules is further pronounced in the *ss3a ss4b* double mutant.[23] Interestingly, knockout of SS3a in wheat leads to deformed A-type granules,[36] but it is not known whether they result from defective initiation or from defects in other processes of starch synthesis. However, genetic studies in Arabidopsis suggest that SS3 can contribute to granule initiation in leaf chloroplasts, where SS3 plays the major role in initiating granules in the absence of SS4.[37,38] It can also exert strong effects on granule morphology, most evident in the *ss3 pii1* mutant, lacking another granule initiation component (MRC/PII1).[39] Overall, the distinct expression pattern of SS3a observed in all examined compound-granule-producing species, combined with the strong effect on compound-granule morphology observed in rice *ss3a* mutants, suggests that differences in SS3a regulation over grain development could be a major factor underpinning variation in granule morphology in grasses.

Although branching enzymes and debranching enzymes are typically associated with amylopectin biosynthesis, SBE1 and LDA are not the major isoforms involved, and thus their exact roles are not clear. It is therefore highly intriguing that these isoforms were highlighted as candidate genes for compound-granule formation in our gene expression dataset. The rice *sbe1* mutant has alterations in amylopectin chain length structure, but this effect is minor compared with mutations in the major isoform—SBE2.[30] Likewise, the rice *lda* (*pul*) mutant has only minor defects in amylopectin chain length structure, compared with mutants in the ISA1 isoform.[29] However, we identified that rice *sbe1* and *lda* (*pul*) mutants had significantly larger granule sizes compared with the wild type—demonstrating that the mutations can also affect granule morphology in a compound-granule-producing species. The increase in size cannot be explained by increased starch content, since neither mutant has altered the total starch content.[29,30] The increased granule size may result from a reduced number of initiations within each compound granule. However, such changes in granule number per amyloplast are difficult to directly quantify. Neither SBE1 nor LDA has previously been implicated in the control of granule number or morphology, but it is plausible that both could be involved. Granule initiation likely requires the branching of maltooligosaccharides to allow the formation of secondary structure and eventually semi-crystalline granules. Indeed, availability of branched maltooligosaccharides influences granule number in Arabidopsis chloroplasts.[40] SBE1 could create branched maltooligosaccharides during early grain development, influencing compound-granule initiation. LDA could also influence this process by generating new linear maltooligosaccharides by releasing them from existing branched glucans, affecting the maltooligosaccharide pool available for granule initiation.

Another candidate gene that showed a rising expression pattern during grain development in all three compound-granule-producing species is GBSS1, which is involved in amylose biosynthesis. Mutants in GBSS1 are known to have drastic reductions in amylose content but have no strong defects in granule morphology in rice.[41] Although there were no general differences in amylose content between the simple- vs. compound-granule-producing species assessed here, it is possible that the two granule types require a different temporal pattern of amylose deposition or that GBSS-binding dynamics to the granule surface are altered. Amylose has also been proposed to affect adhesion between granules,[42] particularly in high-amylose mutants of rice, where compound granules remain more intact during extraction.[43] The possible contribution of GBSS1 to compound-granule formation will need further investigation.

Overall, our phylogenetic and bioinformatic approach to dissect simple vs. compound-granule formation is an important contribution to the understanding of starch biosynthesis, since factors underpinning this variation cannot be studied using genetics alone. Although using wild species was essential to provide multiple examples of species for each morphology class, none of the wild compound-granule-producing species are amenable to genetic transformation, which prevents the generation of knockout mutants for candidate genes directly in these species. We used rice as a model for validating the role of our candidate genes on compound-granule formation, which is genetically amenable but outside the Pooideae clade that we examined in our bioinformatics approach. We cannot rule out that the exact role of these genes differs between rice and the wild Pooideae. Most importantly, our bioinformatics approach

suggested that there are many genes (in addition to SS3a, SBE1, and LDA) that have compound-granule-specific expression patterns, and it is therefore highly unlikely that any single gene would underpin the phenotype. Indeed, knockout of SS3a, SBE1, or LDA all affected granule morphology in rice, including the formation of some simple granules in the *ss3a* mutant, but most granules remained compound in morphology. This suggests that all three genes contribute to the compound-granule morphology but are not solely required for generating that morphology. Consistent with this, numerous forward genetic screens for granule morphology in rice[44,45] have never revealed a mutant that produces primarily simple granules. However, multiple mutants defective in more than one component of starch synthesis can substantially shift granule morphology in barley.[46,47]

Our dataset will continue to be a source of such candidate genes influencing starch granule formation in grass endosperms. Here, we focused on the transcriptional patterns that were common and exclusive to all three compound-granule species compared with the simple-granule species. However, since the selected species represent multiple transitions between the granule types, it is possible that there are also species-specific mechanisms that influence granule morphology. Thus, important genes contributing to granule morphology might also be found by applying a less stringent cutoff, for example, allowing one of the species within each granule type to behave differently from the other two. Indeed, while most starch genes remained stable in expression level in *Brachyelytrum* and *Phaenosperma*, they showed some level of downregulation in *Brachypodium*—demonstrating the diversity in transcriptional patterns of starch genes even among species making the same type of granule morphology. Also, although transcriptomics is a powerful resource for finding gene candidates and is particularly amenable to cross-species comparisons, upregulation of a gene alone does not necessarily indicate a direct role in any given process. It also does not inform about protein abundance or regulation at the biochemical level. For example, starch synthesis proteins in the endosperm are known to undergo protein phosphorylation and/or complex formation, including SBE1 in wheat[48] and SS3a and LDA in rice,[49] which could also contribute to variation in granule morphology. Thus, we cannot rule out other non-transcriptional mechanisms contributing to granule morphology.

RESOURCE AVAILABILITY

Lead contact

Requests for further information and resources should be directed to and will be fulfilled by the lead contact, David Seung (david.seung@jic.ac.uk).

Materials availability

This study did not generate any new genetic lines or reagents. Sources of previously reported transgenic lines are listed in the key resources table.

Data and code availability

- Raw RNA-seq data have been deposited to GenBank under BioProject accession PRJEB91346 and are publicly available as of the date of publication.
- This paper does not report original code.
- Any additional information required to reanalyze the data reported in this paper is available from the lead contact upon request.

ACKNOWLEDGMENTS

We thank JIC Horticultural Services for providing growth facilities and for growing plant material, JIC Bioimaging for providing access to microscopes and expert advice, and JIC Informatics for support with data processing and phylogenetic analyses. We thank the seed banks from which the seed samples were obtained, including the Germplasm Resource Unit of the John Innes Centre, the Millennium Seed Bank at the Royal Botanic Gardens, Kew, and the Germplasm Resources Information Network (GRIN) of the United States Department of Agriculture-Agricultural Research Service (USDA-ARS). We also thank Alastair Lavery for collecting *Nardus* samples, Jonathan D. Monroe (James Madison University) for providing specimens of *Brachyelytrum erectum*, and Martin Röser (Martin Luther University Halle-Wittenberg) for providing seeds of *Amphibromus nervosus*, *Danthoniastrum compactum*, and *Stephanachne nigrescens*. Finally, we thank Steve Kelly (University of Oxford) for providing advice that inspired this study and for valuable guidance on the analysis of the gene expression data. This work was funded through a Leverhulme Trust research project grant RPG-2019-095 (to A.M.S. and D.S.), a Gatsby Foundation grant GAT3587 (to D.S.), a John Innes Foundation (JIF) Chris J. Leaver Fellowship (to D.S.), a Biotechnology and Biological Sciences Research Council (BBSRC, UK) research grant BB/W015935/1 (to D.S.), and BBSRC Institute Strategic Programme grants BB/X01097X/1 and BB/X011003/1 (to the John Innes Centre). A.W.-L. acknowledges internal Harper Adams University funding support.

AUTHOR CONTRIBUTIONS

A.W.-L., A.M.S., and D.S. conceptualized the research and assembled the manuscript (with contributions from all authors); D.F., L.E., A.W.-L., R.M., and D.S. imaged the starch granules; A.W.-L. curated the phylogenetic tree; A.W.-L. analyzed the transcriptomic data; A.W.-L., Q.Y.N., and D.S. carried out the starch extraction and biochemical assays; and N.F., R.M., and D.S. analyzed the rice mutants.

DECLARATION OF INTERESTS

The authors declare no competing interests.

STAR★METHODS

Detailed methods are provided in the online version of this paper and include the following:

- KEY RESOURCES TABLE
- EXPERIMENTAL MODEL AND STUDY PARTICIPANT DETAILS
- METHOD DETAILS
  - Seed development sampling
  - RNA sequencing
  - Bioinformatics
  - Phylogenetic analyses
  - Starch purification
  - Starch content, amylose content and amylopectin chain length analyses
  - Starch size distribution
  - Microscopy
- QUANTIFICATION AND STATISTICAL ANALYSIS

SUPPLEMENTAL INFORMATION

Supplemental information can be found online at https://doi.org/10.1016/j.cub.2026.01.038.

Received: August 12, 2025
Revised: November 16, 2025
Accepted: January 16, 2026
Published: February 13, 2026

REFERENCES

1. Smith, A.M., and Zeeman, S.C. (2020). Starch: A flexible, adaptable carbon store coupled to plant growth. Annu. Rev. Plant Biol. *71*, 217–245. https://doi.org/10.1146/annurev-arplant-050718-100241.
2. Lindeboom, N., Chang, P.R., and Tyler, R.T. (2004). Analytical, biochemical and physicochemical aspects of starch granule size, with emphasis on small granule starches: a review. Starch Stärke *56*, 89–99. https://doi.org/10.1002/star.200300218.
3. Chen, J., Hawkins, E., and Seung, D. (2021). Towards targeted starch modification in plants. Curr. Opin. Plant Biol. *60*, 102013. https://doi.org/10.1016/j.pbi.2021.102013.
4. Li, M., Daygon, V.D., Solah, V., and Dhital, S. (2021). Starch granule size: Does it matter? Crit. Rev. Food Sci. Nutr. *63*, 3683–3703. https://doi.org/10.1080/10408398.2021.1992607.
5. Matsushima, R. (2015). Morphological variations of starch grains. In Starch: Metabolism and Structure, Y. Nakamura, ed. (Springer Japan), pp. 425–441. https://doi.org/10.1007/978-4-431-55495-0_13.
6. Jane, J.L., Kasemsuwan, T., Leas, S., Zobel, H., and Robyt, J.F. (1994). Anthology of starch granule morphology by scanning electron microscopy. Starch Stärke *46*, 121–129. https://doi.org/10.1002/star.19940460402.
7. Tetlow, I.J., and Emes, M.J. (2017). Starch biosynthesis in the developing endosperms of grasses and cereals. Agronomy *7*, 81. https://doi.org/10.3390/agronomy7040081.
8. Yuguchi, Y., Hashimoto, K., Yamamoto, K., Suzuki, S., and Kitamura, S. (2013). Extension of branched chain of amylopectin by enzymatic reaction and its structural characterization. J. Appl. Glycosci. *60*, 131–135. https://doi.org/10.5458/jag.jag.JAG-2012_021.
9. Boyer, C.D., Daniels, R.R., and Shannon, J.C. (1977). Starch granule (amyloplast) development in endosperm of several Zea mays L. genotypes affecting kernel polysaccharides. Am. J. Bot. *64*, 50–56. https://doi.org/10.1002/j.1537-2197.1977.tb07604.x.
10. Myers, A.M., James, M.G., Lin, Q., Yi, G., Stinard, P.S., Hennen-Bierwagen, T.A., and Becraft, P.W. (2011). Maize opaque5 encodes monogalactosyldiacylglycerol synthase and specifically affects galactolipids necessary for amyloplast and chloroplast function. Plant Cell *23*, 2331–2347. https://doi.org/10.1105/tpc.111.087205.
11. Langeveld, S.M., van Wijk, R., Stuurman, N., Kijne, J.W., and de Pater, S. (2000). B-type granule containing protrusions and interconnections between amyloplasts in developing wheat endosperm revealed by transmission electron microscopy and GFP expression. J. Exp. Bot. *51*, 1357–1361. https://doi.org/10.1093/jexbot/51.349.1357.
12. Parker, M.L. (1985). The relationship between A-type and B-type starch granules in the developing endosperm of wheat. J. Cereal Sci. *3*, 271–278. https://doi.org/10.1016/S0733-5210(85)80001-1.
13. Kosina, R., and Grabińska, A. (2016). Variation of starch granules in diploid species of the genus Avena L. modern phytomorphology. Modern Phytomorphology *10*, 9–12. https://doi.org/10.5281/zenodo.159036.
14. Saccomanno, B., Chambers, A.H., Hayes, A., Mackay, I., McWilliam, S.C., and Trafford, K. (2017). Starch granule morphology in oat endosperm. J. Cereal Sci. *73*, 46–54. https://doi.org/10.1016/j.jcs.2016.10.011.
15. Sabelli, P.A., and Larkins, B.A. (2009). The development of endosperm in grasses. Plant Physiol. *149*, 14–26. https://doi.org/10.1104/pp.108.129437.
16. Terrell, E.E. (1971). Survey of occurrences of liquid or soft endosperm in grass genera. Bull. Torrey Bot. Club *98*, 264. https://doi.org/10.2307/2483625.
17. Seung, D., Boudet, J., Monroe, J.D., Schreier, T.B., David, L.C., Abt, M., Lu, K.-J., Zanella, M., and Zeeman, S.C. (2017). Homologs of PROTEIN TARGETING TO STARCH control starch granule initiation in Arabidopsis leaves. Plant Cell *29*, 1657–1677. https://doi.org/10.1105/tpc.17.00222.
18. Watson-Lazowski, A., Raven, E., Feike, D., Hill, L., Barclay, J.E., Smith, A.M., and Seung, D. (2022). Loss of PROTEIN TARGETING TO STARCH 2 has variable effects on starch synthesis across organs and species. J. Exp. Bot. *73*, 6367–6379. https://doi.org/10.1093/jxb/erac268.
19. Hawkins, E., Chen, J., Watson-Lazowski, A., Ahn-Jarvis, J., Barclay, J.E., Fahy, B., Hartley, M., Warren, F.J., and Seung, D. (2021). STARCH SYNTHASE 4 is required for normal starch granule initiation in amyloplasts of wheat endosperm. New Phytol. *230*, 2371–2386. https://doi.org/10.1111/nph.17342.
20. Suh, D.S., Verhoeven, T., Denyer, K., and Jane, J.-L. (2004). Characterization of Nubet and Franubet barley starches. Carbohydr. Polym. *56*, 85–93. https://doi.org/10.1016/j.carbpol.2003.12.005.
21. Chia, T., Chirico, M., King, R., Ramirez-Gonzalez, R., Saccomanno, B., Seung, D., Simmonds, J., Trick, M., Uauy, C., Verhoeven, T., et al. (2020). A carbohydrate-binding protein, B-GRANULE CONTENT 1, influences starch granule size distribution in a dose-dependent manner in polyploid wheat. J. Exp. Bot. *71*, 105–115. https://doi.org/10.1093/jxb/erz405.
22. Fujita, N., Yoshida, M., Kondo, T., Saito, K., Utsumi, Y., Tokunaga, T., Nishi, A., Satoh, H., Park, J.H., Jane, J.L., et al. (2007). Characterization of SSIIIa-deficient mutants of rice: the function of SSIIIa and pleiotropic effects by SSIIIa deficiency in the rice endosperm. Plant Physiol. *144*, 2009–2023. https://doi.org/10.1104/pp.107.102533.
23. Toyosawa, Y., Kawagoe, Y., Matsushima, R., Crofts, N., Ogawa, M., Fukuda, M., Kumamaru, T., Okazaki, Y., Kusano, M., Saito, K., et al. (2016). Deficiency of starch synthase IIIa and IVb alters starch granule morphology from polyhedral to spherical in rice endosperm. Plant Physiol. *170*, 1255–1270. https://doi.org/10.1104/pp.15.01232.
24. Burton, R.A., Jenner, H., Carrangis, L., Fahy, B., Fincher, G.B., Hylton, C., Laurie, D.A., Parker, M., Waite, D., Van Wegen, S., et al. (2002). Starch granule initiation and growth are altered in barley mutants that lack isoamylase activity. Plant J. *31*, 97–112. https://doi.org/10.1046/j.1365-313X.2002.01339.x.
25. Peng, C., Wang, Y., Liu, F., Ren, Y., Zhou, K., Lv, J., Zheng, M., Zhao, S., Zhang, L., Wang, C., et al. (2014). FLOURY ENDOSPERM 6 encodes a CBM48 domain-containing protein involved in compound granule formation and starch synthesis in rice endosperm. Plant J. *77*, 917–930. https://doi.org/10.1111/tpj.12444.
26. Kubo, A., Fujita, N., Harada, K., Matsuda, T., Satoh, H., and Nakamura, Y. (1999). The starch-debranching enzymes isoamylase and pullulanase are both involved in amylopectin biosynthesis in rice endosperm. Plant Physiol. *121*, 399–410. https://doi.org/10.1104/pp.121.2.399.
27. Trafford, K., Haleux, P., Henderson, M., Parker, M., Shirley, N.J., Tucker, M.R., Fincher, G.B., and Burton, R.A. (2013). Grain development in Brachypodium and other grasses: Possible interactions between cell expansion, starch deposition, and cell-wall synthesis. J. Exp. Bot. *64*, 5033–5047. https://doi.org/10.1093/jxb/ert292.
28. Abt, M.R., Pfister, B., Sharma, M., Eicke, S., Bürgy, L., Neale, I., Seung, D., and Zeeman, S.C. (2020). STARCH SYNTHASE5, a noncanonical starch synthase-like protein, promotes starch granule initiation in Arabidopsis. Plant Cell *32*, 2543–2565. https://doi.org/10.1105/tpc.19.00946.
29. Fujita, N., Toyosawa, Y., Utsumi, Y., Higuchi, T., Hanashiro, I., Ikegami, A., Akuzawa, S., Yoshida, M., Mori, A., Inomata, K., et al. (2009). Characterization of pullulanase (PUL)-deficient mutants of rice (Oryza sativa L.) and the function of PUL on starch biosynthesis in the developing rice endosperm. J. Exp. Bot. *60*, 1009–1023. https://doi.org/10.1093/jxb/ern349.
30. Satoh, H., Nishi, A., Yamashita, K., Takemoto, Y., Tanaka, Y., Hosaka, Y., Sakurai, A., Fujita, N., and Nakamura, Y. (2003). Starch-branching enzyme I-deficient mutation specifically affects the structure and properties of starch in rice endosperm. Plant Physiol. *133*, 1111–1121. https://doi.org/10.1104/pp.103.021527.
31. Stoddard, F.L., and Sarker, R. (2000). Characterization of starch in Aegilops species. Cereal Chem. *77*, 445–447. https://doi.org/10.1094/CCHEM.2000.77.4.445.
32. Howard, T., Rejab, N.A., Griffiths, S., Leigh, F., Leverington-Waite, M., Simmonds, J., Uauy, C., and Trafford, K. (2011). Identification of a major

QTL controlling the content of B-type starch granules in Aegilops. J. Exp. Bot. *62*, 2217–2228. https://doi.org/10.1093/jxb/erq423.

33. Dore, W.G. (1956). Some grass genera with liquid endosperm. Bull. Torrey Bot. Club *83*, 335–337. https://doi.org/10.2307/2482798.
34. Seung, D., and Smith, A.M. (2019). Starch granule initiation and morphogenesis-progress in *Arabidopsis* and cereals. J. Exp. Bot. *70*, 771–784. https://doi.org/10.1093/jxb/ery412.
35. Wang, A., Jing, Y., Cheng, Q., Zhou, H., Wang, L., Gong, W., Kou, L., Liu, G., Meng, X., Chen, M., et al. (2023). Loss of function of SSIIIa and SSIIIb coordinately confers high RS content in cooked rice. Proc. Natl. Acad. Sci. USA *120*, e2220622120. https://doi.org/10.1073/pnas.2220622120.
36. Fahy, B., Gonzalez, O., Savva, G.M., Ahn-Jarvis, J.H., Warren, F.J., Dunn, J., Lovegrove, A., and Hazard, B.A. (2022). Loss of starch synthase IIIa changes starch molecular structure and granule morphology in grains of hexaploid bread wheat. Sci. Rep. *12*, 10806. https://doi.org/10.1038/s41598-022-14995-0.
37. Szydlowski, N., Ragel, P., Raynaud, S., Lucas, M.M., Roldán, I., Montero, M., Muñoz, F.J., Ovecka, M., Bahaji, A., Planchot, V., et al. (2009). Starch granule initiation in Arabidopsis requires the presence of either class IV or class III starch synthases. Plant Cell *21*, 2443–2457. https://doi.org/10.1105/tpc.109.066522.
38. Seung, D., Lu, K.-J., Stettler, M., Streb, S., and Zeeman, S.C. (2016). Degradation of glucan primers in the absence of Starch Synthase 4 disrupts starch granule initiation in Arabidopsis. J. Biol. Chem. *291*, 20718–20728. https://doi.org/10.1074/jbc.M116.730648.
39. Vandromme, C., Spriet, C., Putaux, J.L., Dauvillée, D., Courseaux, A., D'Hulst, C., and Wattebled, F. (2023). Further insight into the involvement of PII1 in starch granule initiation in Arabidopsis leaf chloroplasts. New Phytol. *239*, 132–145. https://doi.org/10.1111/nph.18923.
40. Heutinck, A.J.M., Camenisch, S., Fischer-Stettler, M., Sharma, M., Pfister, B., Eicke, S., Liu, C., and Zeeman, S.C. (2025). Branched oligosaccharides cause atypical starch granule initiation in Arabidopsis chloroplasts. Plant Physiol. *197*, kiaf002. https://doi.org/10.1093/plphys/kiaf002.
41. Zhang, C., Zhu, J., Chen, S., Fan, X., Li, Q., Lu, Y., Wang, M., Yu, H., Yi, C., Tang, S., et al. (2019). Wxlv, the ancestral allele of rice Waxy gene. Mol. Plant *12*, 1157–1166. https://doi.org/10.1016/j.molp.2019.05.011.
42. Jiang, H., Horner, H.T., Pepper, T.M., Blanco, M., Campbell, M., and Jane, J.-L. (2010). Formation of elongated starch granules in high-amylose maize. Carbohydr. Polym. *80*, 533–538. https://doi.org/10.1016/j.carbpol.2009.12.016.
43. Wei, C., Xu, B., Qin, F., Yu, H., Chen, C., Meng, X., Zhu, L., Wang, Y., Gu, M., and Liu, Q. (2010). C-type starch from high-amylose rice resistant starch granules modified by antisense RNA inhibition of starch branching enzyme. J. Agric. Food Chem. *58*, 7383–7388. https://doi.org/10.1021/jf100385m.
44. Matsushima, R., Maekawa, M., Kusano, M., Kondo, H., Fujita, N., Kawagoe, Y., and Sakamoto, W. (2014). Amyloplast-localized SUBSTANDARD STARCH GRAIN4 protein influences the size of starch grains in rice endosperm. Plant Physiol. *164*, 623–636. https://doi.org/10.1104/pp.113.229591.
45. Matsushima, R., Maekawa, M., Kusano, M., Tomita, K., Kondo, H., Nishimura, H., Crofts, N., Fujita, N., and Sakamoto, W. (2016). Amyloplast membrane protein SUBSTANDARD STARCH GRAIN6 controls starch grain size in rice endosperm. Plant Physiol. *170*, 1445–1459. https://doi.org/10.1104/pp.15.01811.
46. Matsushima, R., Hisano, H., Galis, I., Miura, S., Crofts, N., Takenaka, Y., Oitome, N.F., Ishimizu, T., Fujita, N., and Sato, K. (2023). FLOURY ENDOSPERM 6 mutations enhance the sugary phenotype caused by the loss of ISOAMYLASE1 in barley. Theor. Appl. Genet. *136*, 94. https://doi.org/10.1007/s00122-023-04339-5.
47. Matsushima, R., Hisano, H., Kim, J.S., McNelly, R., Oitome, N.F., Seung, D., Fujita, N., and Sato, K. (2024). Mutations in starch BRANCHING ENZYME 2a suppress the traits caused by the loss of ISOAMYLASE1 in barley. Theor. Appl. Genet. *137*, 212. https://doi.org/10.1007/s00122-024-04725-7.
48. Tetlow, I.J., Wait, R., Lu, Z., Akkasaeng, R., Bowsher, C.G., Esposito, S., Kosar-Hashemi, B., Morell, M.K., and Emes, M.J. (2004). Protein phosphorylation in amyloplasts regulates starch branching enzyme activity and protein–protein interactions. Plant Cell *16*, 694–708. https://doi.org/10.1105/tpc.017400.
49. Crofts, N., Abe, N., Oitome, N.F., Matsushima, R., Hayashi, M., Tetlow, I.J., Emes, M.J., Nakamura, Y., and Fujita, N. (2015). Amylopectin biosynthetic enzymes from developing rice seed form enzymatically active protein complexes. J. Exp. Bot. *66*, 4469–4482. https://doi.org/10.1093/jxb/erv212.
50. Bolger, A.M., Lohse, M., and Usadel, B. (2014). Trimmomatic: A flexible trimmer for Illumina sequence data. Bioinformatics *30*, 2114–2120. https://doi.org/10.1093/bioinformatics/btu170.
51. Haas, B.J., Papanicolaou, A., Yassour, M., Grabherr, M., Blood, P.D., Bowden, J., Couger, M.B., Eccles, D., Li, B., Lieber, M., et al. (2013). De novo transcript sequence reconstruction from RNA-seq using the Trinity platform for reference generation and analysis. Nat. Protoc. *8*, 1494–1512. https://doi.org/10.1038/nprot.2013.084.
52. Patro, R., Duggal, G., Love, M.I., Irizarry, R.A., and Kingsford, C. (2017). Salmon provides fast and bias-aware quantification of transcript expression. Nat. Methods *14*, 417–419. https://doi.org/10.1038/nmeth.4197.
53. Davidson, N.M., and Oshlack, A. (2014). Corset: enabling differential gene expression analysis for de novo assembled transcriptomes. Genome Biol. *15*, 410. https://doi.org/10.1186/s13059-014-0410-6.
54. Robinson, M.D., McCarthy, D.J., and Smyth, G.K. (2010). edgeR: a Bioconductor package for differential expression analysis of digital gene expression data. Bioinformatics *26*, 139–140. https://doi.org/10.1093/bioinformatics/btp616.
55. Abu-Jamous, B., and Kelly, S. (2018). Clust: automatic extraction of optimal co-expressed gene clusters from gene expression data. Genome Biol. *19*, 172. https://doi.org/10.1186/s13059-018-1536-8.
56. Raudvere, U., Kolberg, L., Kuzmin, I., Arak, T., Adler, P., Peterson, H., and Vilo, J. (2019). g:profiler: A web server for functional enrichment analysis and conversions of gene lists (2019 update). Nucleic Acids Res. *47*, W191–W198. https://doi.org/10.1093/nar/gkz369.
57. Stamatakis, A. (2014). RAxML version 8: a tool for phylogenetic analysis and post-analysis of large phylogenies. Bioinformatics *30*, 1312–1313. https://doi.org/10.1093/bioinformatics/btu033.
58. The International Brachypodium Initiative (2010). Genome sequencing and analysis of the model grass *Brachypodium distachyon*. Nature *463*, 763–768. https://doi.org/10.1038/nature08747.
59. R Development Core Team. (2013). R: A Language and Environment for Statistical Computing (R Foundation for Statistical Computing).
60. Supek, F., Bošnjak, M., Škunca, N., and Šmuc, T. (2011). REVIGO summarizes and visualizes long lists of gene ontology terms. PLoS One *6*, e21800. https://doi.org/10.1371/journal.pone.0021800.
61. Katoh, K., Misawa, K., Kuma, K.I., and Miyata, T. (2002). MAFFT: a novel method for rapid multiple sequence alignment based on fast Fourier transform. Nucleic Acids Res. *30*, 3059–3066. https://doi.org/10.1093/nar/gkf436.
62. Letunic, I., and Bork, P. (2021). Interactive Tree Of Life (iTOL) v5: an online tool for phylogenetic tree display and annotation. Nucleic Acids Res. *49*, W293–W296. https://doi.org/10.1093/nar/gkab301.
63. Yamamoto, K., Sawada, S., and Onogaki, T. (1973). Properties of rice starch prepared by alkali method with various conditions. J. Jpn. Soc. Starch Sci. *20*, 99–104. https://doi.org/10.5458/jag1972.20.99.
64. Yamamoto, K., Sawada, S., and Onogaki, T. (1981). Effects of quality and quantity of alkali solution on the properties of rice starch. J. Jpn. Soc. Starch Sci. *28*, 241–244. https://doi.org/10.5458/jag1972.28.241.
65. Seung, D., Echevarría-Poza, A., Steuernagel, B., and Smith, A.M. (2020). Natural polymorphisms in Arabidopsis result in wide variation or loss of the amylose component of starch. Plant Physiol. *182*, 870–881. https://doi.org/10.1104/pp.19.01062.

66. Zeeman, S.C., Tiessen, A., Pilling, E., Kato, K.L., Donald, A.M., and Smith, A.M. (2002). Starch synthesis in Arabidopsis. Granule synthesis, composition, and structure. Plant Physiol. *129*, 516–529. https://doi.org/10.1104/pp.003756.

67. Streb, S., Delatte, T., Umhang, M., Eicke, S., Schorderet, M., Reinhardt, D., and Zeeman, S.C. (2008). Starch granule biosynthesis in Arabidopsis is abolished by removal of all debranching enzymes but restored by the subsequent removal of an endoamylase. Plant Cell *20*, 3448–3466. https://doi.org/10.1105/tpc.108.063487.

68. Matsushima, R., Maekawa, M., Fujita, N., and Sakamoto, W. (2010). A rapid, direct observation method to isolate mutants with defects in starch grain morphology in rice. Plant Cell Physiol. *51*, 728–741. https://doi.org/10.1093/pcp/pcq040.

STAR★METHODS

KEY RESOURCES TABLE

REAGENT or RESOURCE	SOURCE	IDENTIFIER
Chemicals, peptides, and recombinant proteins		
α-amylase (*Aspergillus oryzae*)	Megazyme	E-ANAAM
Amyloglucosidase (*Aspergillus niger*)	Roche	10102857001
Hexokinase (from yeast overproducer)	Roche	11426362001
glucose-6-phosphate dehydrogenase (from *Leuconostoc mesenteroides*)	Roche	10165875001
isoamylase (*Pseudomonas* sp.)	Megazyme	E-ISAMY
pullulanase (*Klebsiella planticola*)	Megazyme	E-PULKP
Lugol's solution	Sigma-Aldrich	62650
Periodic Acid Schiff (PAS) Stain	Abcam	ab150680
Deposited data		
Alignment used for Figure 1 phylogenetic tree	This study	Zenodo 10.5281/zenodo.18259798
RNAseq reads	This study	NCBI PRJEB91346
Experimental models: Organisms/strains		
Achnatherum calamagrostis	Chiltern Seeds, Wallingford, UK	N/A
Achnatherum hymenoides (*Stipa hymenoides*)	The Sainsbury Laboratory, Norwich, UK	N/A
Aegilops comosa	John Innes Centre, Norwich, UK	N/A
Agropyron cristatum	The Sainsbury Laboratory, Norwich, UK	N/A
Agrostis capillaris	Emorsgate Seeds, Wisbech, UK	N/A
Alopecurus geniculatus	Emorsgate Seeds, Wisbech, UK	N/A
Alopecurus pratensis	Emorsgate Seeds, Wisbech, UK	N/A
Amelichloa brachychaeta	USDA-ARS Western Regional PI, Washington, USA	PI 197978
Ampelodesmos mauritanicus	B&T World Seeds, Paguignan, France	N/A
Amphibromus nervosus (*Hook. f.*) *Baillon*	Halle University, Germany	N/A
Anthoxanthum odoratum	Emorsgate Seeds, Wisbech, UK	N/A
Arrhenatherum elatius	Emorsgate Seeds, Wisbech, UK	N/A
Avena abyssinica	The Sainsbury Laboratory, Norwich, UK	N/A
Avena sativa	John Innes Centre, Norwich, UK	N/A
Avenella flexuosa	USDA-ARS Western Regional PI, Washington, USA	PI 283244
Beckmannia syzigachne	USDA ARS Plant Genetic Resources Conservation Unit, Georgia, USA	PI 610658
Bellardiochloa variegata	USDA-ARS Western Regional PI, Washington, USA	PI 253455
Brachyelytrum erectum	James Madison University, USA	N/A
Brachyelytrum japonicum	Plant World Seeds, Devon, UK	N/A
Brachypodium distachyon	John Innes Centre, Norwich UK	N/A
Brachypodium pinnatum	The Plantsman's Preference, Diss, UK	N/A
Brachypodium sylvaticum	Emorsgate Seeds, Wisbech, UK	N/A
Briza media	The Sainsbury Laboratory, Norwich, UK	N/A
Bromopsis erecta	Emorsgate Seeds, Wisbech, UK	N/A
Bromus catharticus var. catharticus	USDA-ARS Western Regional PI, Washington, USA	W6 10415
Bromus hordeaceus	Emorsgate Seeds, Wisbech, UK	N/A
Bromus japonicus	The Sainsbury Laboratory, Norwich, UK	N/A
Calamagrostis arundinacea	Kew Millennium Seed Bank, Wakehurst, UK	62859/645948
Calamagrostis brachytricha	Plant World Seeds, Devon, UK	N/A
Calamagrostis canescens	Kew Millennium Seed Bank, Wakehurst, UK	135805

(*Continued on next page*)

Continued

REAGENT or RESOURCE	SOURCE	IDENTIFIER
Calamagrostis foliosa	Kew Millennium Seed Bank, Wakehurst, UK	201966
Calamagrostis inexpansa	Kew Millennium Seed Bank, Wakehurst, UK	201520
Calamagrostis nutkaensis	Kew Millennium Seed Bank, Wakehurst, UK	171580
Calamagrostis scopulorum	Kew Millennium Seed Bank, Wakehurst, UK	561123
Catapodium marinum	Kew Millennium Seed Bank, Wakehurst, UK	53132/163583/807139
Cinna arundinacea	USDA-ARS Western Regional PI, Washington, USA	W6 49641
Colpodium humile	USDA-ARS Western Regional PI, Washington, USA	PI 598593
Cynosurus cristatus	The Sainsbury Laboratory, Norwich, UK	N/A
Dactylis glomerata	The Sainsbury Laboratory, Norwich, UK	N/A
Danthoniastrum compactum	Halle University, Germany	N/A
Dasypyrum villosum	The Sainsbury Laboratory, Norwich, UK	N/A
Deschampsia cespitosa	Emorsgate Seeds, Wisbech, UK	N/A
Diarrhena obovata	B&T World Seeds, Paguignan, France	N/A
Dichelachne crinita	USDA-ARS Western Regional PI, Washington, USA	W6 22474
Echinaria capitata	The Sainsbury Laboratory, Norwich, UK	N/A
Elymus aristiglumis	USDA-ARS Western Regional PI, Washington, USA	PI 598486
Elymus canadensis	USDA-ARS Western Regional PI, Washington, USA	PI 634291
Elymus dahuricus	USDA-ARS Western Regional PI, Washington, USA	PI 611025
Elymus macrochaetus	USDA-ARS Western Regional PI, Washington, USA	PI 611000
Elymus magellanicus	Plant World Seeds, Devon, UK	N/A
Elymus nutans	USDA-ARS Western Regional PI, Washington, USA	PI 678451
Elymus semicostatus	USDA-ARS Western Regional PI, Washington, USA	PI 203242
Elymus sibiricus	USDA-ARS Western Regional PI, Washington, USA	PI 598371
Elymus trachycaulus	USDA-ARS Western Regional PI, Washington, USA	PI 598468
Festuca ovina	Emorsgate Seeds, Wisbech, UK	N/A
Festuca pratensis (Schedonorus pratensis)	The Sainsbury Laboratory, Norwich, UK	N/A
Festuca rubra	Emorsgate Seeds, Wisbech, UK	N/A
Hesperostipa comata	USDA-ARS Western Regional PI, Washington, USA	W6 32648
Hierochloe odorata	Chiltern Seeds, Wallingford, UK	N/A
Holcus lanatus	The Sainsbury Laboratory, Norwich, UK	N/A
Hordeum jubatum	John Innes Centre, Norwich, UK	N/A
Hordeum secalinum	Emorsgate Seeds, Wisbech, UK	N/A
Jarava plumosa	USDA-ARS Western Regional PI, Washington, USA	PI 203787
Koeleria macrantha	Emorsgate Seeds, Wisbech, UK	N/A
Lagurus ovatus	Chiltern Seeds, Wallingford, UK	N/A
Lolium perenne	The Sainsbury Laboratory, Norwich, UK	N/A
Lygeum spartum	Kew Millennium Seed Bank, Wakehurst, UK	105167/185109
Macrochloa tenacissima	USDA-ARS Western Regional PI, Washington, USA	PI 239234
Melica altissima	The Plantsman's Preference, Diss, UK	N/A
Melica ciliata	The Sainsbury Laboratory, Norwich, UK	N/A
Milium effusum	Chiltern Seeds, Wallingford, UK	N/A
Nardus stricta	Collected from Woodland Trust Hill in Perthshire, Scotland	N/A
Nassella hyalina	USDA-ARS Western Regional PI, Washington, USA	PI 197867
Nephelochloa orientalis	USDA-ARS Western Regional PI, Washington, USA	W6 19223
Oloptum miliaceum	USDA-ARS Western Regional PI, Washington, USA	PI 187143
Oryza sativa cv. Nipponbare	Fujita et al.[22,29]	N/A
Oryza sativa cv. Nipponbare *pul* mutant	Fujita et al.[29]	N/A
Oryza sativa cv. Nipponbare *ss3a* mutant	Fujita et al.[22]	N/A

(*Continued on next page*)

Continued		
REAGENT or RESOURCE	SOURCE	IDENTIFIER
Oryza sativa cv. Taichung 65 (T65)	Satoh et al.[30]	N/A
Oryza sativa cv. Taichung 65 (T65) *sbe1* mutant	Satoh et al.[30]	N/A
Oryzopsis pubiflora	USDA-ARS Western Regional PI, Washington, USA	PI 228355
Phaenosperma globosa	The Plantsman's Preference, Diss, UK	N/A
Phalaris coerulescens	The Sainsbury Laboratory, Norwich, UK	N/A
Phleum bertolonii	Emorsgate Seeds, Wisbech, UK	N/A
Piptatheropsis canadensis	USDA-ARS Western Regional PI, Washington, USA	PI 236875
Piptatherum songaricum	USDA-ARS Western Regional PI, Washington, USA	PI 598562
Poa trivialis	The Sainsbury Laboratory, Norwich, UK	N/A
Ptilagrostis mongholica	USDA-ARS Western Regional PI, Washington, USA	PI 676207
Puccinellia distans	USDA-ARS Western Regional PI, Washington, USA	PI 600922
Puccinellia maritima	USDA-ARS Western Regional PI, Washington, USA	PI 260702
Secale anatolicum	The Sainsbury Laboratory, Norwich, UK	N/A
Secale cereale	John Innes Centre, Norwich UK	N/A
Secale iranicum	The Sainsbury Laboratory, Norwich, UK	N/A
Secale momtanum	The Sainsbury Laboratory, Norwich, UK	N/A
Secale vavilovii	The Sainsbury Laboratory, Norwich, UK	N/A
Stephanachne nigrescens	Halle University, Germany	N/A
Stipa arabica	USDA-ARS Western Regional PI, Washington, USA	PI 275367
Stipa calamagrostis	Kew Millennium Seed Bank, Wakehurst, UK	51080/67049/961815
Stipa caragana	Kew Millennium Seed Bank, Wakehurst, UK	694131/775014
Stipa caucasica subsp. desertorum	USDA-ARS Western Regional PI, Washington, USA	PI 665577
Stipa lagascae	USDA-ARS Western Regional PI, Washington, USA	PI 204737
Stipa offneri	USDA-ARS Western Regional PI, Washington, USA	PI 287941
Stipa ucrainica	USDA-ARS Western Regional PI, Washington, USA	PI 314114
Stipellula capensis	USDA-ARS Western Regional PI, Washington, USA	PI 170808
Thinopyrum bessarabicum	The Sainsbury Laboratory, Norwich, UK	N/A
Thinopyrum elongatum	The Sainsbury Laboratory, Norwich, UK	N/A
Thinopyrum intermedium	The Sainsbury Laboratory, Norwich, UK	N/A
Thinopyrum ponticum	The Sainsbury Laboratory, Norwich, UK	N/A
Thinopyrum turcicum	The Sainsbury Laboratory, Norwich, UK	N/A
Ventenata macra	USDA-ARS Western Regional PI, Washington, USA	PI 204431
Software and algorithms		
Trimmomatic	Bolger et al.[50]	N/A
Trinity	Haas et al.[51]	N/A
Transdecoder	Haas et al.[51]	N/A
Salmon	Patro et al.[52]	N/A
Corset	Davidson et al.[53]	N/A
EdgeR	Robinson et al.[54]	N/A
Clust	Abu-Jamous et al.[55]	N/A
g:Profiler	Raudvere et al.[56]	N/A
RaxML	Stamatakis et al.[57]	N/A

EXPERIMENTAL MODEL AND STUDY PARTICIPANT DETAILS

For starch granule morphology classification, seed samples from various species of the Pooideae subfamily were obtained from different sources and were directly analyzed without regrowing (key resources table; Table S1). The six species that were grown and further characterised in this study (*Brachyelytrum japonicum*, *Brachypodium distachyon*, *Calamagrostis brachytricha*, *Melica altissima*, *Nardus stricta*, and *Phaenosperma globosa*) were cultivated as follows: Two species, *Brachypodium* and *Melica*, were grown

in a controlled environment chamber (MLR-352H, PHCbi, Breda, The Netherlands) at 60% relative humidity and a light intensity of 150 μmol photons m^{-2} s^{-1}, with 16 h light at 24°C and 8 h dark at 18°C. For the other four species, due to large plant sizes and the requirement for seasonal natural cycles for flowering, plants were grown in a glasshouse at the John Innes Centre in Norwich, United Kingdom (52.622192° N, 1.221695° E) without supplemental lighting, with a minimum daytime/night time temperature of 18°C/16°C. Plants were grown in glasshouse conditions for at least 10 months before flowering between 2019 and 2021. All plants were grown in JIC Cereal Mix compost (65% peat, 25% loam, 10% grit, 3 kg/m^3 dolomitic limestone, 1.3 kg/m^3 Yara PG mix, 3 kg/m^3 Osmocote exact).

METHOD DETAILS

Seed development sampling

As soon as anthers were visible, tillers were labelled as 0 days post anthesis (DPA). Seed was collected at 3, 6, 9 and 14 DPA for each species. For each collection, spikelets were harvested then immediately snap frozen in liquid nitrogen and stored at -80°C. Sampling was carried out 5-6 hours after sunrise (or equivalent time in the controlled environment chamber). Individual seeds were extracted while on dry ice, and the correct developmental stage was confirmed prior to further analyses.

RNA sequencing

Outer seed coats were removed from extracted seeds on dry ice. The lemma (if present) was not removed to limit damage to the seed and avoid excessive thawing. RNA was extracted from pooled seeds (8-10 seeds per biological replicate for 3 and 6 DPA, 4-5 seeds per biological replicate for 9 and 14 DPA) using the RNeasy PowerPlant kit (Qiagen), incorporating an on-column DNase digest. Following quality control, library preparation with poly-A selection was carried out at Novogene (Cambridge, UK). RNA-sequencing was then carried out on a NovaSeq 6000 machine (Illumina), returning ~30 million 150 base pair paired end reads per sample.

Bioinformatics

Raw reads were first filtered to remove reads with adapter contamination or low quality using Trimmomatic.[50] The filtered reads from species without a published transcriptome were assembled into a *de novo* assembly using Trinity.[51] Each *de novo* assembly contained a set of non-redundant contiguous sequences (contigs) that could be used as a reference transcriptome. Summary statistics for each *de novo* assembly can be found in Data S3A. For contig annotation, candidate coding regions were first identified using Transdecoder.[51] All candidate coding regions were then annotated to the *Brachypodium distachyon* v3.1 proteome via BLASTp. Once all annotations were retrieved, the *aggregate* function in R was used to identify the consensus annotation for each contig.

Filtered reads were aligned to their relevant transcriptome using the quasialign mode within Salmon.[52] This returned both raw counts and a relative transcript abundance for each transcript/contig (transcripts per million; TPM). For the *de novo* assembled transcriptomes, contigs were hierarchically clustered based on expression and shared reads using Corset,[53] and then these clusters combined based on annotation, to produce aggregated count values suitable for statistical testing. EdgeR[54] was then used to identify significantly differentially expressed transcripts/clusters (significance cut-offs of FDR $\leq$ 0.05 and $\log_2$ fold change > 1.5) with a minimum count cut-off of 1 count per million in at least three replicates. *For Brachypodium*, the *Brachypodium distachyon* v3.1 reference transcriptome[58] was directly used for mapping. Filtered reads were aligned to the reference transcriptome as above, producing raw counts directly suitable for statistical testing (as above) and TPM values for each gene. The average TPM values for each species and timepoint can be found in Data S3.

Principal component analyses (PCA) were carried out in R using the prcomp function and then plotted using the ggbiplot package.[59] A cut-off of $\geq$ 1 TPM for each sample within a species was used for a gene to be included in the PCA. Clustering analyses were performed using *Clust*,[55] using the in-built normalisation for TPM values as the input and a tightness value of 5. Filtering was set as a minimum of 10 TPM in total in one condition to be included in the analysis. Clustering was performed using either all species (all species), only simple granules species (simple), or only compound granule species (compound). Significantly overrepresented gene ontology (GO) categories (Adj. P-value $\leq$ 0.05) were calculated using g:Profiler.[56] Disposable GO categories (those also represented by a child GO term) were identified using REVIGO and removed to reduce redundancy.[60]

Phylogenetic analyses

Sequences of NADH dehydrogenase F (*ndhF*) and Maturase K (*matK*) were extracted from NCBI for each species. For each gene, the collected nucleotide sequences were aligned using MAFFT translational align with a 1.53 gap penalty, a 0.123 offset value, the G-INS-i algorithm and the BLOSUM62 scoring matrix.[61] As some sequences were partial, aligned sequences were trimmed to regions available for all species, ensuring the sequences remained in the correct reading frame, to prevent missing data from confounding our analyses. This resulted in total fragment sizes of 582 bp and 792 bp for *ndhF* and *matK*, respectively. Sequences were then combined, and a final alignment was made using the same parameters as above (Alignment available on Zenodo: 10.5281/zenodo.18259798). The phylogenetic tree was built from this alignment using RaxML,[57] with a GTR CAT model and 1000 bootstrap replicates, selecting the best scoring maximum likelihood tree. The phylogenetic tree was visualised and curated using iTOL.[62]

Starch purification

For starch purification from Pooideae grass seeds: Mature seeds were soaked overnight in 0.5 mL ddH_2O at 4°C, then homogenized in a ball mill (Retsch MM-300) at 30 Hz, 1 min. The homogenates were filtered through a 60 μm nylon mesh then centrifuged at 3,000*g*, 5 min. The pellet was resuspended in ddH_2O and centrifuged at 2500*g*, 5 min, over a cushion of 90% (v/v) Percoll, 50 mM Tris-HCl, pH 8. The pellet was then washed twice in 50 mM Tris-HCl, pH 6.8, 10 mM EDTA, 4% SDS (v/v), 10 mM DTT, removing any remaining debris using selective resuspension. Finally, the pellet was washed twice with ddH_2O.

For starch purification from rice: Starch granules were prepared from polished rice following the cold-alkali method.[63,64] Seeds were harvested from paddy fields and 200 grains of rice were pooled for each starch purification.

Starch content, amylose content and amylopectin chain length analyses

Several seeds per biological replicate were collected and weighed. As seeds were limited for *Nardus*, seeds from three biological replicates were pooled into a single sample. Seeds were ground in a ball mill (Retsch MM-300), and the powdered sample was extracted in 0.7 M perchloric acid. The extracts were centrifuged at 20,000*g*, and the pellet was then washed three times in 80% (v/v) ethanol, followed by resuspension in water. This is the "resuspended pellet" that is used for the starch content, amylose content and amylopectin chain length below. All enzymes used in these analyses are in the key resources table:

Starch content was quantified using the hexokinase/glucose-6-phosphate dehydrogenase method.[17] An aliquot of resuspended pellet was gelatinized at 95°C for 15 min, and subsequently digested in 105 mM sodium acetate buffer, pH 4.8, using α-amylase (Megazyme, 1 U) and amyloglucosidase (Roche, 1.3 U) at 37°C for 2 h. Starch content (in glucose equivalents) was determined via a glucose assay using a hexokinase/glucose-6-phosphate dehydrogenase-based spectrophotometric method (Roche). The assay was carried out in a 200 μL reaction in 50 mM HEPES-NaOH, pH 7.5, 1 mM $MgCl_2$, 1 mM ATP, 1 mM NAD, 1.4 U hexokinase and 0.5 U glucose-6-phosphate dehydrogenase, and NADH production was monitored on a plate spectrophotometer at 340 nm. A standard curve of glucose was produced for quantification.

Amylose content was quantified using iodine colorimetry.[65] An aliquot of resuspended pellet (equivalent to 50 μg starch as quantified above) was gelatinized at 95°C for 10 min then filtered through a 20 μm nylon mesh. The filtrate was mixed with Lugol's solution (KI/I_2; Sigma) at a ratio of 10:1 (filtrate:Lugol's). The absorbance spectrum between 500-750 nm was measured using a spectrophotometer. Amylose content was quantified using the absorbance values at 525 nm (A_{525}) and 700 nm (A_{700}) with the equation of Zeeman et al.[66]:

$$\text{Amylose \%} = (3.039 - (7.154(A_{700}/A_{525}))/(3.048(A_{700}/A_{525}) - 19.129) \times 100$$

For amylopectin chain length distribution analysis, an aliquot of resuspended pellet (equivalent to 100 μg starch as quantified above) was gelatinised at 95°C for 15 min before debranching with isoamylase (Megazyme, 0.02 U) and pullulanase (Megazyme, 1 U) in 10 mM sodium acetate, pH 4.8. The debranched starch was purified over sequential columns of AmberChrom 50WX4 and 1X4 (both 200-400 mesh), then analyzed by High Performance Anion Exchange Chromatography with Pulsed Amperometric Detection on a Dionex ICS-5000-PAD fitted with a PA-200 column (Thermo). Separation gradient was made using eluent A (100 mM NaOH) and eluent B (150 mM NaOH and 500 mM sodium acetate) as previously described[67]: 0 to 13 min, a linear gradient from 95% A and 5% B to 60% A and 40% B; 13 to 50 min, a linear gradient to 15% A and 85% B; 50 to 70 min, step to 95% A and 5% B. Flow rate was set to 0.25 mL/min.

Starch size distribution

For analysis of granule size distributions, the starch was suspended into Isoton II (Beckman Coulter, Brea, CA, USA), and relative volume vs. diameter plots were generated using a Multisizer 4e Coulter counter (Beckman Coulter) with a 70 μm aperture tube. A minimum of 80,000 particles was measured per sample. All measurements were conducted with logarithmic bin spacing but are presented on a linear x-axis for clarity.

Microscopy

Granule morphology was assessed using scanning electron microscopy (SEM). Dry mature seeds were cracked or cut open and were mounted onto stubs. Stubs were sputter coated with gold prior to imaging in a Nova NanoSEM 450 (FEI). For purified starch, granules were dried directly onto the mount before sputter coating and imaging as above. For developing grains, segments were excised from approximately halfway along the length of the seed (at 3-, 6-, 9- and 14-days post anthesis (DPA)) and fixed as above. Using an EM TP embedding machine (Leica, Milton Keynes, UK), samples were post-fixed in 1% (w/v) OsO_4 in 0.05 M sodium cacodylate for 1 h at room temperature, dehydrated in ethanol and infiltrated with LR White resin (London Resin Company). LR White blocks were polymerized at 60°C and semi-thin sections (~0.5 μm) were taken from the blocks. Sections were stained with the Periodic Acid Schiff (PAS) Stain Kit (Abcam) with the following staining times: 30 mins in the Periodic Acid solution, and 5 mins in the Schiff's reagent. This was followed by staining with 0.5% (w/v) toluidine blue for 30 seconds, prior to mounting in Histomount. Sections were imaged with a DM6000 (Leica) microscope.

Observations of starch granules in sections of mature rice grains were done as described previously.[68] Cubic blocks of ~1 mm were cut from the central region of the endosperm of mature, dry seeds and fixed in a solution containing 5% (v/v) formalin, 5% (v/v) acetic acid, and 50% (v/v) ethanol for at least 12 h at room temperature. Samples were then dehydrated through a graded ethanol series [30, 50, 70, 90 and 100 % (v/v)] and then embedded in Technovit 7100 resin (Kulzer GmbH, Germany). Semi-thin sections (approximately 1 μm) were prepared using a diamond knife (Diatome AG, Ultra trim, 3.0 mm, Switzerland) set on an

ultramicrotome (Leica Microsystems, LEICA EM UC7, Germany), and dried onto coverslips. These were stained with 40-fold diluted Lugol solution and subsequently examined under a microscope (Olympus, BX53, Japan).

QUANTIFICATION AND STATISTICAL ANALYSIS

One-way ANOVA tests were used in R to assess significant differences in phenotypic traits across species. For mean granule size, either a one-way ANOVA or pairwise t-test was used to compare the mutant phenotype against the relevant wild type. Each variable was first tested for normality using the Shapiro–Wilks test before analysis, then, if necessary, transformed using the log or squared function in R. Where suitable, if a significance value of ≤ 0.05 was returned, a Tukey post-hoc test was used to identify which species were significantly different. The type of test, number of replicates, and the nature of the replication used for individual experiments are indicated in the figure legends.